

Sven Grützmacher
Fritz-Frey-Str. 2
69121 Heidelberg
sven[at]endstage.net

Mat.-Nr.: 2864128

Deformations of flags and convex sets in $\mathbb{R}P^2$

Masterarbeit in Mathematik
Ruprecht-Karls-Universität Heidelberg
Fakultät für Mathematik & Informatik
Mathematisches Institut

Supervisor: Prof. Dr. Anna Wienhard
Dr. Gye-Seon Lee

This thesis was created using \LaTeX and the KOMA-scripts.

Abstract

Deformation spaces have always been of importance in geometry. By understanding how objects change one can also find properties that help understand if two objects are the same in a certain sense, e.g. two triangles in the euclidian plane are the same if there is an isometry sending one onto the other.

In this thesis we want to investigate deformations of n -tuples of flags in the projective plane and provide visualizations of the changes. This will allow us to parameterize the space of positive n -tuples of flags by considering internal parameters induced by a triangulation of suitably nested polygons. By introducing the eruption, shearing and bulging flows discussed by Wienhard and Zhang [WZ18] we are then able to fully understand and visualize how these parameters change.

We will also draw a connection to hyperbolic geometry through showing that ideal polygons in properly convex sets are of finite volume with regard to the Hilbert metric. Furthermore we will extend the deformations to marked strictly convex domains with C^1 boundary.

But the main goal of this thesis remains to visualize the deformations in some of the discussed cases.

Deformationsräume waren immer schon von Wichtigkeit in der Geometrie. Wenn man versteht wie sich Objekte verändern, dann kann man dabei auf Eigenschaften treffen welche Objekte auch unterscheidbar machen, zum Beispiel sind zwei Dreiecke in der euklidischen Ebene gleich, falls eine Isometrie existiert welche das eine auf das andere abbildet.

In dieser Arbeit wollen wir Deformationen von n -Tupeln von Flaggen in der projektiven Ebene untersuchen und dazu Visualisierungen bereitstellen. Durch das betrachten interner Parameter, induziert durch eine Triangulierung von passend verschachtelten Polygonen, können wir somit den Raum der positiven Flaggen- n -Tupeln parametrisieren. Mit den von Wienhard und Zhang [WZ18] eingeführten bulging, shearing und eruption flows wird es uns gelingen die Veränderungen in den internen Parametern zu verstehen und zu visualisieren.

Wir werden außerdem eine Verbindung zur hyperbolischen Geometrie herstellen indem wir zeigen, dass ideale Polygone in eigentlich konvexen Mengen auch ein endliches Volumen bezüglich der Hilbertmetrik haben. Des weiteren wollen wir die Deformation von Flaggen auf strikt konvexe Mengen mit C^1 Rand erweitern.

Das Hauptziel dieser Arbeit bleibt jedoch das Visualisieren der Deformationen in den betrachteten Fällen.

Acknowledgements

I would like to thank

Anna Wienhard

for giving me the opportunity to write this thesis and for bringing interesting maths to Heidelberg. It really kept me staying.

Gye-Seon Lee

for supporting me greatly throughout my thesis and all the seminars before.

저는 Gye-Seon Lee에게 그가 주었던 그간의 모든 도움과 유익했던 미팅들에 대하여 감사하고 싶습니다. 그의 피드백과 도움은 언제나 나에게 옳은 방향을 제시해 주었습니다.

Dominik and Tim

for finding many mistakes and giving valuable tips.

Jasmina

for supporting me throughout these stressful times and always giving me a shoulder to rest on. Also for proof-reading and spotting countless missing points.

Erklärung zur Masterarbeit

Ich versichere hiermit, dass ich diese Arbeit selbstständig verfasst habe und keine anderen
als die angegebenen Quellen und Hilfsmittel benutzt habe.

Die Arbeit habe ich bisher keinem anderen Prüfungsamt in gleicher oder vergleichbarer
Form vorgelegt.

Heidelberg, den

Sven Grützmacher

Contents

1	Introduction	1
2	Preliminaries	5
2.1	Projective Space	5
2.2	Cross ratio	6
2.3	Flags and Triple ratio	9
2.4	Suitably nested polygons	13
3	Properly convex sets in \mathbb{RP}^2	19
3.1	Tilings of \mathbb{S}^n	20
3.2	Convexity	23
3.3	Examples	24
3.4	Construction using flags, finite volume polygons	28
3.4.1	Construction	28
3.4.2	Finite volume	29
3.5	Examples	33
4	Deformations of convex sets in \mathbb{RP}^2	35
4.1	Flag deformations	35
4.1.1	Triples in \mathcal{F}_3^+	35
4.1.2	Quadruples in \mathcal{F}_4^+	37
4.1.3	n -tuples in \mathcal{F}_n^+	42
4.2	Deformations of convex sets	47
4.2.1	With C^1 -boundary (general)	47
4.2.2	Constructed from tilings	52
5	Visualization	59
5.1	\mathbb{RP}^2 and affine charts	59
5.2	Convex sets in \mathbb{RP}^2 from tilings	60
5.3	Convex sets in \mathbb{RP}^2 from flags	62
	List of Figures	i
	Bibliography	iii

1 Introduction

The study of convex real projective structures on a closed connected orientable surface of genus $g \geq 2$ has been pioneered by Bill Goldman [Gol90]. In recent years, Wienhard and Zhang built on this foundation and discussed flows on the space of convex real projective structures which are described by explicit deformations of the internal parameters associated to each pair of pants in a pants decomposition [WZ18]. They built upon the work of Fock-Goncharov [FG07], who parameterized the space of n -tuples of flags in \mathbb{R}^3 using internal parameters defined by cross and triple ratios. He did this by drawing a connection between positive tuples of flags and suitably nested polygons. Using this connection Wienhard and Zhang described the eruption, shearing and bulging flows in the context of n -tuples of positive flags and then extended these flows to the setting of marked strictly convex domains with C^1 -boundary. Their initial motivation was to develop an understanding of how a generalization of the earthquake theorem from the context of Teichmüller spaces could look like in the space of convex real projective structures.

The aim of this thesis is to recall the work of Wienhard and Zhang up to the deformations of convex sets in \mathbb{RP}^2 with C^1 -boundary while providing more details and visualizations for the flows.

Consider a positive n -tuple of flags $F = ((p_1, l_1), \dots, (p_n, l_n)) \in \mathcal{F}_n^+$ together with its corresponding pair of suitably nested polygons (N, N') . Choosing a triangulation of N we obtain a set of internal edges $a_{i,j}$ between p_i and p_j as well as a set of triangles $T_{i,j,k}$ with vertices p_i, p_j, p_k . Then we can make use of the projective invariants, i.e. the triple and cross ratio to define coordinates on \mathcal{F}_n^+ via:

$$\begin{aligned}\sigma_{i,j}(F) &= \log \left(-C(l_i, p_k, p_{k'}, \overline{p_i p_j}) \right), \quad i < k < j < k' < i, \\ \tau_{i,j,k}(F) &= \log \left(T((p_i, l_i), (p_j, l_j), (p_k, l_k)) \right), \quad i < j < k < i.\end{aligned}$$

This will allow us to parameterize \mathcal{F}_n^+ . Let $I_{\mathcal{T}}$ be the set of internal edges for a triangulation \mathcal{T} and $\Theta_{\mathcal{T}}$ be the set of triangles.

Theorem. Let $m = 2 \cdot \#I_{\mathcal{T}} + \#\Theta_{\mathcal{T}}$. The map

$$\left((\sigma_{i,j}, \sigma_{j,i})_{a_{i,j} \in I_{\mathcal{T}}}, (\tau_{i,j,k})_{T_{i,j,k} \in \Theta_{\mathcal{T}}} \right) : \mathrm{PGL}(3, \mathbb{R}) \setminus \mathcal{F}_n^+ \longrightarrow \mathbb{R}^m$$

is a homeomorphism.

Keeping this in mind we will show how to construct convex sets in \mathbb{RP}^2 by using the Vinberg theorem [Ben09, Theorem 1.5]. Vinberg gave sufficient conditions on when a convex polygon in \mathbb{S}^2 tiles some convex domain.

Theorem (Vinberg). Let P be a convex polygon of \mathbb{S}^2 and, for each edge s of P , let $R_s = \text{Id} - \alpha_s \otimes v_s$ be a projective reflection fixing the face s . Let $a_{s,t} = \alpha_s(v_t)$ and suppose that conditions

1. $a_{s,t} \leq 0$ and $(a_{s,t} = 0 \Leftrightarrow a_{t,s} = 0)$,
2. $a_{s,t}a_{t,s} = 4$ or $a_{s,t}a_{t,s} = 4 \cos^2\left(\frac{\pi}{m_{s,t}}\right)$ with integer $m_{s,t} \geq 2$,

are satisfied for every s, t such that $\text{codim}(s \cap t) = 2$. Let Γ be the group generated by the reflections R_s . Then

- a) the polygons $\gamma(P)$, for $\gamma \in \Gamma$, tile some convex subset C of \mathbb{S}^2 ,
- b) the group Γ is discrete in $\text{SL}^\pm(3, \mathbb{R})$.

Using this we can construct convex sets in two ways. On the one hand we will consider tilings by triangles in \mathbb{S}^2 and on the other hand the tilings obtained from a suitably nested polygon of an element $F \in \mathcal{F}_n^+$. From the latter approach we will be able to draw a connection to hyperbolic geometry because the inner polygon N will be an ideal polygon in the constructed convex set Ω . Furthermore, the Hilbert metric on Ω will induce a measure μ_Ω . In this setting we have

Theorem. Let $F = (F_1, \dots, F_n) \in \mathcal{F}_n^+$ and (N, N') be a pair of suitably nested polygons. Let Ω be the convex set constructed from N . Then, with regard to the Hilbert metric on Ω , $\mu_\Omega(N) < \infty$.

Concerning the deformations we can define the eruption flow on \mathcal{F}_3^+ which will change the internal parameter corresponding to the triple ratio. The parameters coming from the cross ratio will change by the bulging and shearing flows initially defined on \mathcal{F}_4^+ . To generalize these deformations of \mathcal{F}_n^+ we observe that choosing an internal edge of a triangulation on N will also split the both N and N' into two components. Also, choosing a triangle in the triangulation, we split N and N' into a triangle and three more polygons. These constructions allow us to directly generalize the flows from \mathcal{F}_3^+ and \mathcal{F}_4^+ to \mathcal{F}_n^+ .

To generalize the deformations to a convex set Ω with C^1 -boundary we can observe that by choosing points on $\partial\Omega$ together with the tangents at these points we obtain flags. This is a general approach and is used to understand marked strictly convex domains with C^1 -boundary.

If, on the other hand, a convex set Ω was constructed from a pair of suitably nested polygons (N, N') we have two additional ways to define the flows on Ω . Either we transform N and construct a new Ω' from this polygon or we apply the deformation on every piece in the tiling. In these cases this assures us that the group action which was used to construct these sets also acts on Ω' . We can see that, using the right transformations both approaches will yield the same result.

This thesis is organized as follows. In Chapter 2, we recall properties of some classical projective invariants, namely the cross ratio and the triple ratio on triples of flags. In Chapter 3 we describe two ways to generate properly convex sets in the projective plane and provide examples and graphical assistance. Here we will also draw the connection to hyperbolic geometry

by showing that ideal polygons are of finite volume with regard to the Hilbert metric in these cases. Using the constructions from Chapter 3 we discuss the various deformations in Chapter 4 and also extend them from flags to properly convex sets in \mathbb{RP}^2 . In the last chapter we will give a few tips on how to visualize certain things.

Throughout this thesis we will provide graphical assistance and visualizations of the various constructions and deformations.

2 Preliminaries

Before we start with the in-depth theory of deforming properly convex sets we introduce some needed basics for this thesis. We start by introducing the projective plane and its dual. Afterwards we take a look at two projective invariants which will help us distinguish certain objects later on. First we consider the cross ratio of four lines or points in \mathbb{RP}^2 with suitable properties. Then we define flags in the projective plane by which we can consider the triple ratio on triples of flags.

We will continue to investigate a geometric property of n-tuples of flags, that is the existence of certain nested polygons which will also be of importance later on. The chapter will end by giving a parametrization for a subset of the space of n-tuples of flags called the positive flags. We closely follow [WZ18], but provide more details and graphical assistance.

2.1 Projective Space

First of all we define the mathematical space this thesis will mostly take place in, the projective plane.

Definition 2.1.1. The **projective line** \mathbb{RP}^1 is the set of all 1-dimensional subspaces in \mathbb{R}^2 . The **projective plane** \mathbb{RP}^2 is the set of all 1-dimensional subspaces in \mathbb{R}^3 .

Therefore it is also clear that each hyperplane in \mathbb{R}^3 corresponds to a projective line in the projective plane. The following two results are characteristic for the projective setting.

Proposition 2.1. *Given two points $p, q \in \mathbb{RP}^2$ with $p \neq q$ there is a unique projective line through p and q .*

Given two lines $k, l \subset \mathbb{RP}^2$ with $k \neq l$ there is a unique intersection point.

Proof. Since $p \neq q$ they span a unique hyperplane which projects to a unique line in \mathbb{RP}^2 .

Also two lines in \mathbb{RP}^2 correspond to two hyperplanes in \mathbb{R}^3 . Because they are not equal they intersect in a single line corresponding to a unique point in the projective plane. \square

Now we also know that we can identify \mathbb{RP}^2 as the quotient $(\mathbb{R}^3 \setminus \{0\}) / \mathbb{R}^\times$, meaning that for $x, y \in \mathbb{R}^3 \setminus \{0\}$ we have $x \sim y \Leftrightarrow x = \lambda y$ for some $\lambda \neq 0$. Thus we can always choose a representative $x \in \mathbb{R}^3$. We will denote the class of x in the projective plane by $[x]$. Note that we will often just write x or (x_1, x_2, x_3) instead of $[x_1, x_2, x_3]$ as it should be clear from the context in which setting we are.

For later we want to take a short look at the dual projective plane:

Definition 2.1.2. The **dual projective plane** \mathbb{RP}^{2*} is $\mathbb{P}((\mathbb{R}^3)^*)$, i.e. the space of all 1-dimensional subspaces in the dual of \mathbb{R}^3 .

Analogous to the above observations it is clear that the dual can be seen as a quotient space. There is a nice identification regarding projective lines and elements of the dual plane.

Proposition 2.2. *There is a bijection between points in \mathbb{RP}^{2*} and projective lines in \mathbb{RP}^2 given by*

$$f \in \mathbb{RP}^{2*} \mapsto \ker f.$$

Proof. Let $[f] \in \mathbb{RP}^{2*}$. Then $\ker f$ is a hyperplane in \mathbb{R}^3 and thus a line in \mathbb{RP}^2 . Because $\ker(\lambda f) = \ker(f)$ for $\lambda \neq 0$ the map is well-defined.

Take a line $l \subset \mathbb{RP}^2$. This corresponds to a hyperplane $P \subset \mathbb{R}^3$. Now choose an element $f \in (\mathbb{R}^3)^*$ such that $P = \ker f$. Note that if $P = \ker g$ for a $g \in (\mathbb{R}^3)^*$ then $g = \lambda f$, $\lambda \neq 0$. Thus, we have the bijection between l and the class $[f]$. \square

We see that under this identification the condition $l(p) = 0$ is equivalent to p lying on the line l . To make use of this fact we introduce the following notation.

Definition 2.1.3. The set \mathcal{L}_n is the set of pairwise distinct n -tuples $l_1, \dots, l_n \in \mathbb{RP}^{2*}$ such that there exists some $p \in \mathbb{RP}^2$ so that $l_i(p) = 0$ for all $i = 1, \dots, n$.

Given the above identification this set identifies with n -tuples of lines which intersect in a common point.

It is also important to take a look at projective transformations

Definition 2.1.4. A **projective transformation** of \mathbb{RP}^2 is an element of $\text{GL}(3, \mathbb{R})/\mathbb{R}^\times$, i.e. an invertible matrix up to scaling by non-zero real numbers.

The **group of projective transformations** will be denoted by $\text{PGL}(3, \mathbb{R})$. Since it is clear that these are equivalence classes we will simply write A instead of $[A]$.

The following observation may be useful later on: for any map $A \in \text{PGL}(3, \mathbb{R})$ we have a unique representative in $\text{SL}(3, \mathbb{R})$ via the bijection

$$\text{PGL}(3, \mathbb{R}) \longrightarrow \text{SL}(3, \mathbb{R}), \quad A \mapsto \frac{1}{\det(A)^{1/3}} A.$$

2.2 Cross ratio

Because we understand the surrounding space now we start to consider two projective invariants needed in the following sections. The first is the well-known cross ratio of four points that lie on a line. We approach this ratio from a dual point of view and start by considering tuples of points.

Definition 2.2.1. An n -tuple of points $p_1, \dots, p_n \in \mathbb{RP}^2$ is called **generic** if no triple of the points lie on a projective line.

We denote the set of all generic n -tuples by \mathcal{P}_n .

We now take a look at a well-known property of projective transformations to give a little motivation for the invariants we want to define.

Proposition 2.3 (see [Boy]). *For every pair of $n+2$ points in \mathbb{RP}^n such that no $n+1$ are linearly dependent there is a unique projective transformation sending one onto the other.*

In our case this boils down to

Proposition 2.4. *For every pair of generic 4-tuple in \mathbb{RP}^2 there is a unique projective transformation sending one to the other, i.e. $\text{PGL}(3)$ acts transitively on \mathcal{P}_4 .*

But what happens if the 4-tuple is non-generic? By the above general version of the proposition we can surely find a transformation sending 3 points on a projective line onto 3 other points on a line. In general, using 4 points, the action may not be transitive any more. Yet there are still several subsets in \mathcal{P}_4 where we have conditions on when the action is transitive, e.g. when all four points lie on a projective line.

Since we lack a metric for now, we start by defining an invariant for elements in \mathcal{L}_4 , i.e. certain tuples of lines instead of tuples of points.

Definition 2.2.2. The **cross ratio** is the function $C : \mathcal{L}_4 \longrightarrow \mathbb{R} \setminus \{0, 1\}$ given by

$$C(l_1, l_2, l_3, l_4) = \frac{l_1(p_3) \cdot l_4(p_2)}{l_1(p_2) \cdot l_4(p_3)},$$

for points $p_2, p_3 \in \mathbb{RP}^2 \setminus \{p\}$ which lie on l_2 and l_3 respectively and p is the common intersection point of all four lines.

Naturally we have to choose representatives α_i for the l_i and v_j for the p_j to compute the cross ratio in each case. Luckily the value of C does not depend on the choice of those representatives.

Proposition 2.5. *C is well defined.*

Proof. It is clear that choosing, for example, $\lambda\alpha_1$ as a representative for l_1 does not change the value of C . If we know choose a point $q_2 = p + t \cdot p_2$ with $t \neq 0$ on l_2 we get

$$\begin{aligned} C(l_1, l_2, l_3, l_4) &= \frac{l_1(p_3) \cdot l_4(p + tp_2)}{l_1(p + tp_2) \cdot l_4(p_3)} \\ &= \frac{l_1(p_3) \cdot l_4(p) + l_1(p_3) \cdot l_4(tp_2)}{l_1(p) \cdot l_4(p_3) + l_1(tp_2) \cdot l_4(p_3)} \\ &= \frac{l_1(p_3) \cdot l_4(p_2)}{l_1(p_2) \cdot l_4(p_3)}, \end{aligned}$$

since $l_i(p) = 0$ and $l_i(tp_j) = tl_i(p_j)$. □

So from now on we will simply write l_i instead of α_i . It should be clear from the context what happens.

We also state some properties of the cross ratio that are well-known

Proposition 2.6. *Let $(l_1, l_2, l_3, l_4) \in \mathcal{L}_4$. Then*

a) $C(l_1, l_2, l_3, l_4) = \frac{1}{C(l_1, l_3, l_2, l_4)} = 1 - C(l_2, l_1, l_3, l_4) = C(l_4, l_3, l_2, l_1),$

b) C is invariant under the action of $\text{PGL}(3, \mathbb{R})$,

c) C is surjective and its level sets are the $\text{PGL}(3, \mathbb{R})$ -orbits in \mathcal{L}_4 .

Proof. a) The first equality just exchanges numerator and denominator and the last one is obvious.

For the second equality we will, to show this once, choose representatives α_i, v_j and v for p .

Because C is well defined we may choose $v_3 = sv_1 + tv_2$. Then

$$\begin{aligned} \frac{\alpha_1(v_3) \cdot \alpha_4(v_2)}{\alpha_1(v_2) \cdot \alpha_4(v_3)} + \frac{\alpha_2(v_3) \cdot \alpha_4(v_1)}{\alpha_2(v_1) \cdot \alpha_4(v_3)} &= \frac{t\alpha_1(v_2) \cdot \alpha_4(v_2)}{\alpha_1(v_2) \cdot \alpha_4(v_3)} + \frac{s\alpha_2(v_1) \cdot \alpha_4(v_1)}{\alpha_2(v_1) \cdot \alpha_4(v_3)} \\ &= \frac{\alpha_4(tv_2 + sv_1)}{\alpha_4(v_3)} = 1. \end{aligned}$$

b) First of all, from linear algebra we know that if the $(p_i)_i$ are transformed by $g \in \text{PGL}(3, \mathbb{R})$, i.e. $p_i \mapsto gp_i$, then the $(l_i)_i$ transform via $l_i \mapsto l_i g^{-1}$. Thus, for example $l_1(p_3) \mapsto l_1 g^{-1} g p_3 = l_1(p_3)$. This proves the claim.

c) Again choose all four points on one line. Then there is $t \notin \{0, 1\}$ such that $p_2 = (1-t)p_1 + tp_4$. Then, in the basis p_1, p, p_4 we get

$$C(l_1, l_2, l_3, l_4) = \frac{(1-t)d}{tc}.$$

So C is surjective. Now assume to have two elements $(l_1, l_2, l_3, l_4), (l'_1, l'_2, l'_3, l'_4) \in \mathcal{L}_4$ with $C(l_1, l_2, l_3, l_4) = C(l'_1, l'_2, l'_3, l'_4)$. Choosing p_i on a line and also a suitable bases we know there is a $g \in \text{PGL}(3)$ such that $gp = p'$ and $gp_i = p'_i$ for $i = 1, 2, 4$. From b) and the fact that the cross ratios are the same we now know the ratio $d/c = d'/c'$ and by linear algebra g also sends p_3 to p'_3 . So two elements in \mathcal{L}_4 are the same modulo $\text{PGL}(3, \mathbb{R})$ if and only if their cross ratios are the same. □

We also want to define the cross ratio for four points lying in a projective line. For this we consider the following corollary

Corollary 2.7. *Let p_1, \dots, p_4 be four points on a projective line l and let q, q' be two distinct points of which both do not lie on l . Let l_i and l'_i be the lines through p_i and q or q' respectively. Then*

$$C(l_1, l_2, l_3, l_4) = C(l'_1, l'_2, l'_3, l'_4)$$

Proof. This follows directly from b) of the previous proposition. Note that we can always find a map $g \in \text{PGL}(3, \mathbb{R})$ sending q, p_1, \dots, p_4 to q', p_1, \dots, p_4 since four of those points lie on a line. □

With this we can define

$$C(p_1, p_2, p_3, p_4) = C(l_1, l_2, l_3, l_4) \tag{2.1}$$

Next we see if we can define a notion of a metric on certain subsets of \mathbb{RP}^2 . For this we consider convex subsets. Note that the topology on \mathbb{RP}^2 is the quotient topology on $(\mathbb{R}^3 \setminus \{0\}) / \mathbb{R}^\times$.

Definition 2.2.3. A domain $\Omega \subset \mathbb{RP}^2$ is called **properly convex** if it is open, any two points can be connected by a projective line segment and the closure does not contain any projective line.

A properly convex domain is called **strictly convex** if $\partial\Omega$ does not contain any nontrivial line segments.

Through this we can make use of the cross ratio to define a metric:

Definition 2.2.4. Let $\Omega \subset \mathbb{RP}^2$ be a properly convex domain. For any two points $p, q \in \Omega$ let $a, b \in \partial\Omega$ be the points so that a, p, q, b lie on a projective line in \mathbb{RP}^2 in that order. Then the **Hilbert metric** is the function

$$d_\Omega : \Omega \times \Omega \longrightarrow \mathbb{R}; \quad (p, q) \mapsto \log |C(a, p, q, b)|.$$

We leave it to the reader to check that this is truly a metric. It is worth noting that d_Ω is invariant under projective transformations that leave Ω invariant. Also the literature often defines the metric with a coefficient of $\frac{1}{2}$. This makes the metric coincide with the hyperbolic metric on the unit disk. For details consider [BK53, Chapter IV. 28].

2.3 Flags and Triple ratio

We now introduce the main object of this thesis, a flag. We then proceed to introduce a projective invariant for triples of flags by which we can also extract a special subset, namely the positive flags. The section will end by giving a geometric interpretation of positive flags.

Definition 2.3.1. A **flag** is a pair $(p, l) \in \mathbb{RP}^2 \times \mathbb{RP}^{2*}$ so that $l(p) = 0$. Two flags $(p, l), (q, k)$ are **transverse** if $l(q) \neq 0 \neq k(p)$. The set of ordered pairwise transverse n -tuples of flags is denoted by \mathcal{F}_n .

Identifying elements in \mathbb{RP}^{2*} with projective lines, a flag is a line together with a point on it and two flags are transverse if their designated points do not lie on the other line.

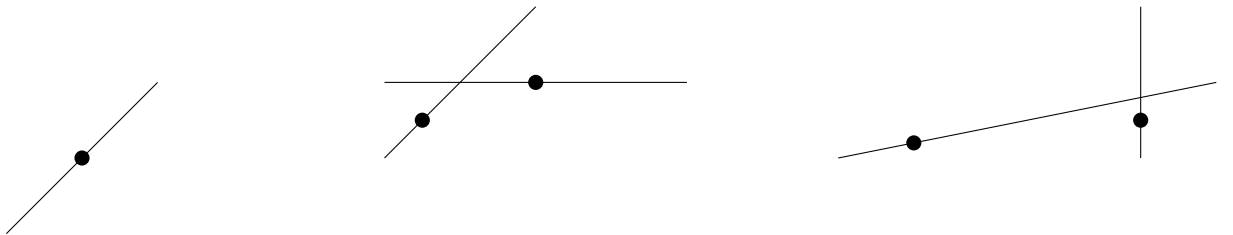


Figure 2.1: A flag and two pairs of transverse flags.

Like with the cross ratio we want to build a projective invariant for a certain class of flags, in this case for \mathcal{F}_3 .

Definition 2.3.2. The **triple ratio** is the function $T : \mathcal{F}_3 \longrightarrow \mathbb{R} \setminus \{0\}$ defined by

$$T((p_1, l_1), (p_2, l_2), (p_3, l_3)) = \frac{l_1(p_2)l_2(p_3)l_3(p_1)}{l_1(p_3)l_3(p_2)l_2(p_1)}.$$

As with the cross ratio we have to take representatives of each class, but it is also easy to see that the triple ratio does not depend on those choices. Let us now take a look at some properties.

Proposition 2.8. *Let $(F_1, F_2, F_3) \in \mathcal{F}_3$. Then*

a)
$$T(F_1, F_2, F_3) = \frac{1}{T(F_1, F_3, F_2)},$$

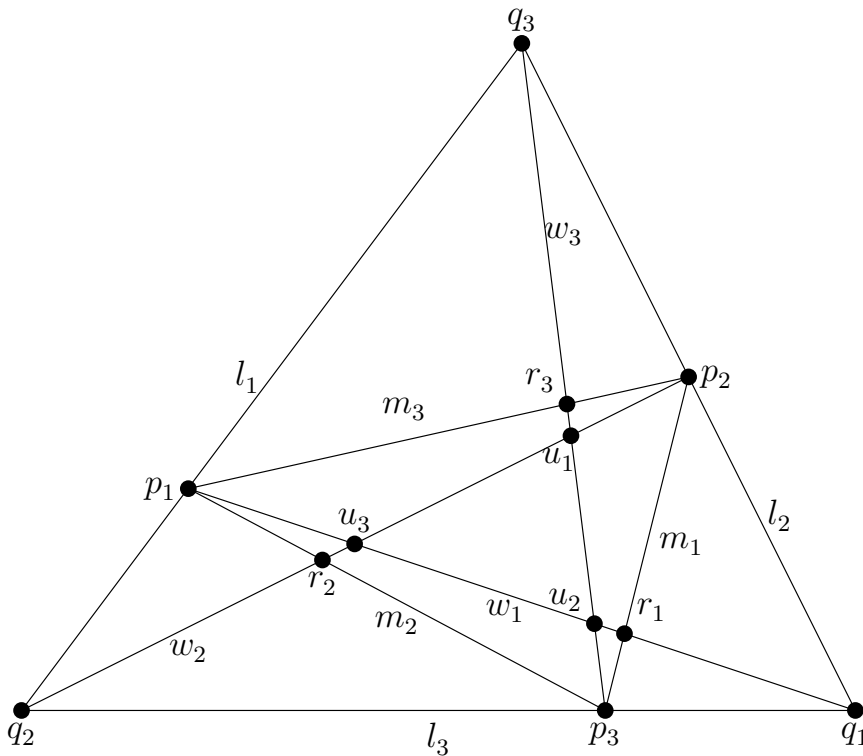
b) *For any $g \in \text{PGL}(3)$ we have $T(F_1, F_2, F_3) = T(gF_1, gF_2, gF_3)$,*

c) *T is surjective and its level sets are the $\text{PGL}(3)$ -orbits in \mathcal{F}_3 .*

Proof. a) Take the reciprocal

b) Again because of $l_i(p_j) \mapsto l_i g^{-1} g p_j = l_i(p_j)$ the claim follows directly.

c) From b) it is easy to see that the value of T can be changed by simply sliding the points on the line. Thus T is surjective. If you take two elements in \mathcal{F}_3 with the same triple ratio take the q_i, q'_i for $i = 1, 2, 3$ and p_1, p'_1 . Then there is a unique $g \in \text{PGL}(3)$ that sends $q_i \mapsto q'_i$ and $p_1 \mapsto p'_1, p_2 \mapsto p'_2$. Since the coordinates of p_3 and p'_3 have each the same ratio and the triple ratio is the same, g also maps $p_3 \mapsto p'_3$. This concludes the proof. □



$t_2 \bullet$

Figure 2.2: Important notation for cross/triple ratio in \mathcal{F}_3 (t_1, t_3 omitted).

It is now time to describe a relationship between triple and cross ratios which will yield a geometric interpretation of the triple ratio. For this we need some notation:

Notation 2.3.3. Let $((p_1, l_1), (p_2, l_2), (p_3, l_3)) \in \mathcal{F}_3$ and again let $i, j, k = 1, 2, 3$ be pairwise distinct. Set $q_k = l_i \cap l_j$ and let m_k be the projective line through p_i, p_j . Set w_k to be the line through p_k and q_k , $t_k = l_k \cap m_k$ and $r_k = w_k \cap m_k$. Lastly set $u_k = w_i \cap w_j$. We will do all the subscript arithmetic modulo 3.

Using this we can compute that

Proposition 2.9. For the above naming and notation $p_i, u_{i-1}, u_{i+1}, q_i$ lie on a line and

$$C(p_i, u_{i-1}, u_{i+1}, q_i) = T(F_1, F_3, F_2)$$

for all $i = 1, 2, 3$.

Proof. We can again choose coordinates such that q_i are a basis which results in

$$l_i = e_i^T \quad p_1 = \begin{pmatrix} 0 \\ a \\ b \end{pmatrix} \quad p_2 = \begin{pmatrix} c \\ 0 \\ d \end{pmatrix} \quad p_3 = \begin{pmatrix} e \\ f \\ 0 \end{pmatrix}$$

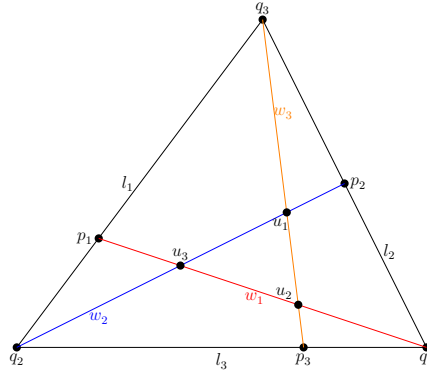


Figure 2.3: Cross ratio connected to triple ratio

Then a short computation gives us (for example $w_1(p_1) = 0 = w_1(q_1)$)

$$w_1 = [0, b, -a] \quad w_2 = [-d, 0, c] \quad w_3 = [f, -e, 0]$$

Their intersection points lie in the classes

$$u_1 = \left[1, \frac{f}{e}, \frac{d}{c}\right]^T \quad u_2 = \left[\frac{e}{f}, 1, \frac{b}{a}\right]^T \quad u_3 = \left[\frac{c}{d}, \frac{a}{b}, 1\right]^T$$

It is easy to check that the necessary points really lie on a line. Plugging this in our formulas we deduce

$$C(p_i, u_{i-1}, u_{i+1}, q_i) = \frac{ade}{cfb} = T(F_1, F_3, F_2).$$

□

For later purposes we can, by using the sign of the triple ratio, define a particular subset of \mathcal{F}_3 or in general of \mathcal{F}_n .

Definition 2.3.4. A n-tuple $(F_1, \dots, F_n) \in \mathcal{F}_n$ is called **positive** if $T(F_i, F_j, F_k) > 0$ for all triples $i < j < k < i$ in the cyclic order.

We denote the set of positive triples by $\mathcal{F}_n^+ \subset \mathcal{F}_n$.

There are two ways to give a geometric meaning to this property in \mathcal{F}_3 for a triple $F = (F_1, F_2, F_3)$:

- i) let again $i, j, k = 1, 2, 3$ be pairwise distinct and let r_k and t_k as in notation 2.3.3. Then $F > 0$ if and only if r_k and t_k lie in distinct connected components of $\mathbb{RP}^2 \setminus (l_i \cup l_j)$,
- ii) $F > 0$ if and only if there is a triangle Δ with vertices p_1, p_2, p_3 and a triangle Δ' with edges l_1, l_2, l_3 such that $\Delta \subset \Delta'$. Note that by triangle we mean 2-simplex, i.e. not just the boundary.

To see i) consider for example $k = 1$

Choose a basis and representatives as in proposition 2.9. Then

$$t_1 = \begin{bmatrix} 0 \\ -\frac{cf}{ed} \\ 1 \end{bmatrix} \quad r_1 = \begin{bmatrix} \frac{ade+bcf}{bdf} \\ \frac{a}{b} \\ 1 \end{bmatrix}$$

which gives us

$$l_3(t_1) = 1 = l_3(r_1)$$

$$l_2(t_1) = -\frac{cf}{ed} = -T(F_1, F_2, F_3) \frac{a}{b}$$

$$l_2(r_1) = \frac{a}{b}$$

So the latter have different signs if and only if $T(F_1, F_2, F_3) > 0$.

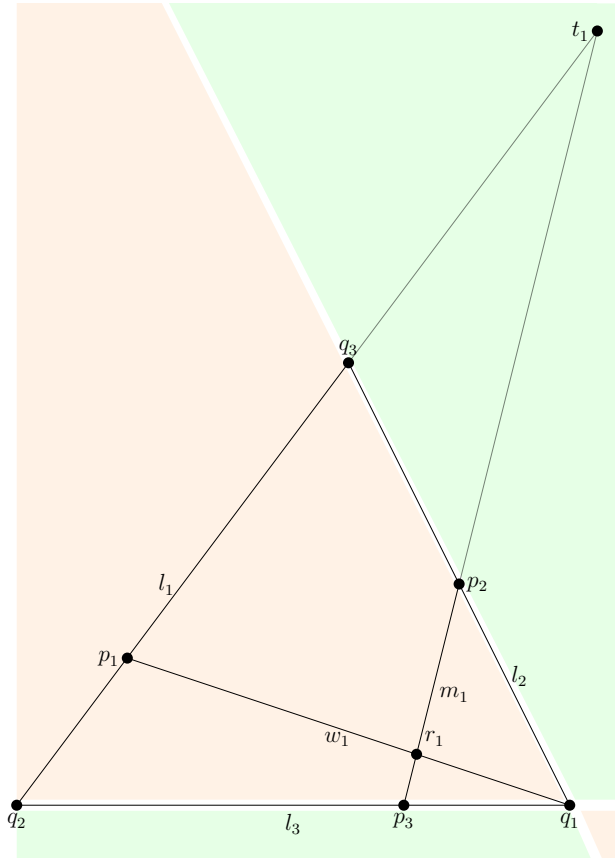


Figure 2.4: $0 < F \in \mathcal{F}_3$ and coloured components of $\mathbb{RP}^2 \setminus (l_2 \cup l_3)$

We will consider ii) later in a more general setting. To make a last observation we denote the parts of Δ, Δ' like in the picture below so that

$$\Delta = T \cup T_1 \cup T_2 \cup T_3$$

$$\Delta' = T \cup Q_1 \cup Q_2 \cup Q_3$$

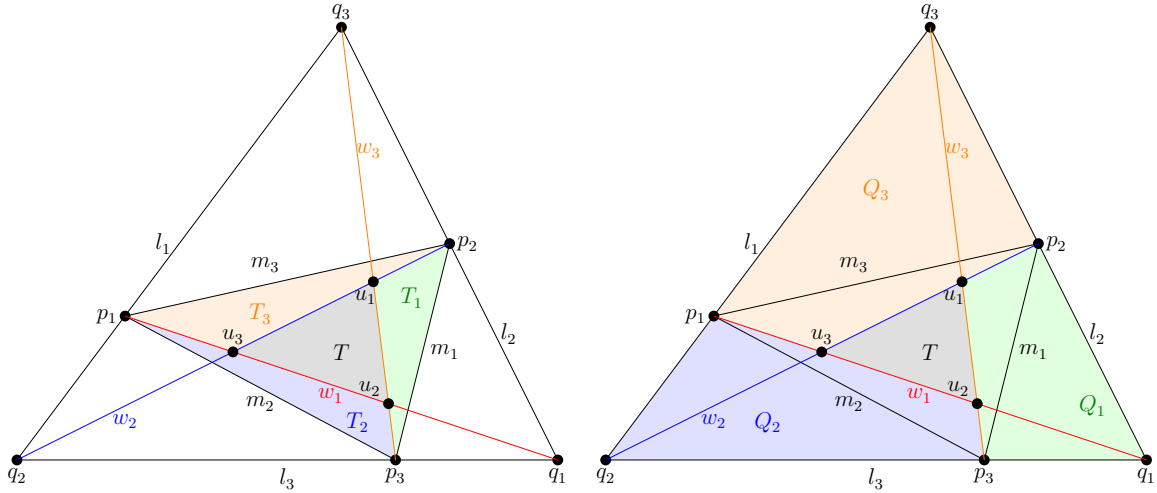


Figure 2.5: nested triangles and decomposition for triple of flags

Using this notation we can make an observation about the triangle T

Corollary 2.10. *Let $(F_1, F_2, F_3) = ((p_1, l_1), (p_2, l_2), (p_3, l_3)) \in \mathcal{F}_3^+$ and let Δ' be as above. Then $\log T(F_1, F_3, F_2)$ is the Hilbert length of the side of the triangle T with respect to the properly convex set Δ' . In particular T is an equilateral triangle with respect to this metric.*

2.4 Suitably nested polygons

In this section we draw a connection between positive flags and suitably nested polygons and try to explicitly parametrize \mathcal{F}_n^+ using projective invariants.

Definition 2.4.1. i) A **polygon** in \mathbb{RP}^2 is a properly convex and compact set in \mathbb{RP}^2 whose boundary is a union of finitely many projective line segments. Those segments are the **edges** and the endpoints are the **vertices**.

ii) A **labelled polygon** is a polygon equipped with an ordering on its vertices, so that the successor of any vertex v in this ordering is connected to v by an edge.

iii) We denote the vertices of a labelled polygon N as $p_1(N), \dots, p_n(N)$ and the edges $e_1(N), \dots, e_n(N)$ such that $e_i(N)$ has endpoints $p_i(N), p_{i+1}(N)$.

iv) A pair (N, N') of labelled n -gons is suitably nested if and only if $N \subset N'$ and $p_i(N)$ lies in the interior of $e_i(N')$.

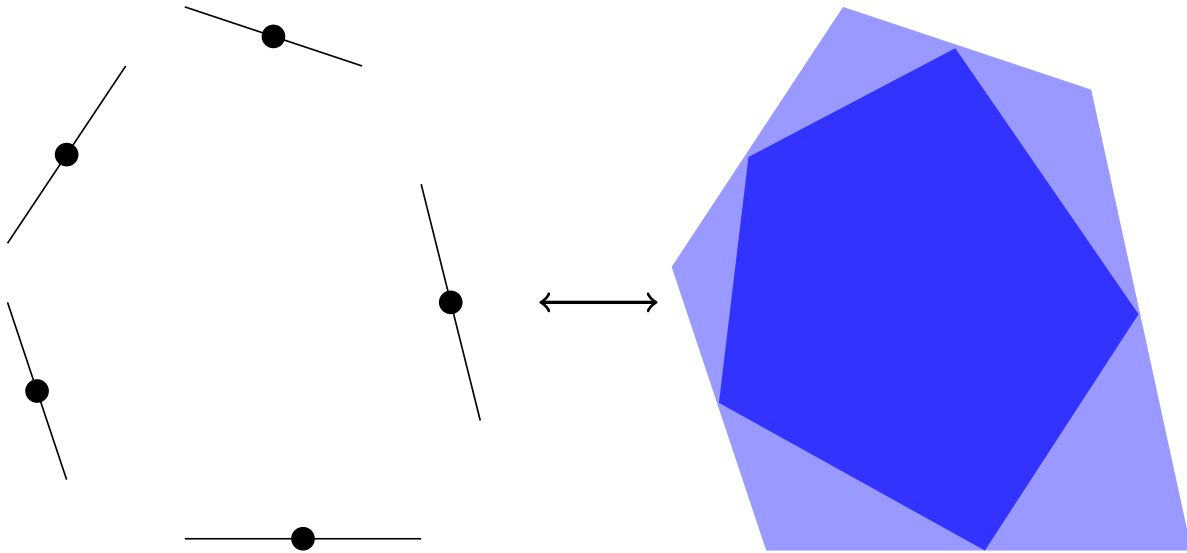


Figure 2.6: Suitably nested polygons with corresponding flags.

Proposition 2.11. *Let $((p_1, l_1), \dots, (p_n, l_n)) = F \in \mathcal{F}_n$, $n \geq 3$. Then $F \in \mathcal{F}_n^+$ if and only if there is a pair of suitably nested labelled n -gons (N, N') so that $p_i(N) = p_i$ and $e_i(N') \subset l_i$.*

Proof. To prove this we will take three steps:

- 1) Let $F \in \mathcal{F}_3$ and choose the basis $(q_i)_i$. Then there are s, t, r such that

$$\begin{aligned} p_1 &= tq_2 + (1 - t)q_3 \\ p_2 &= sq_3 + (1 - s)q_1 \\ p_3 &= rq_1 + (1 - r)q_2 \end{aligned}$$

Then

$$T(F_1, F_2, F_3) = \frac{(1 - t)(1 - s)(1 - r)}{tsr}$$

From this it is easy to check that the theorem holds. For example (see the picture on the right) assume $T > 0$ and without loss of generality that $0 < r < 1$. Then if $s \in (0, 1)$ it follows directly that $t \in (0, 1)$ (red) and otherwise we have $s, t \in [0, 1]^C$.

Note that the green area is also a triangle with vertices q_1, q_2, q_3 .

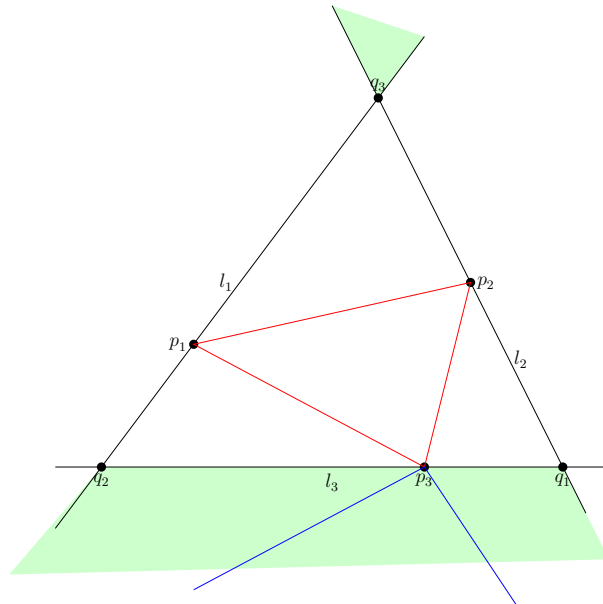
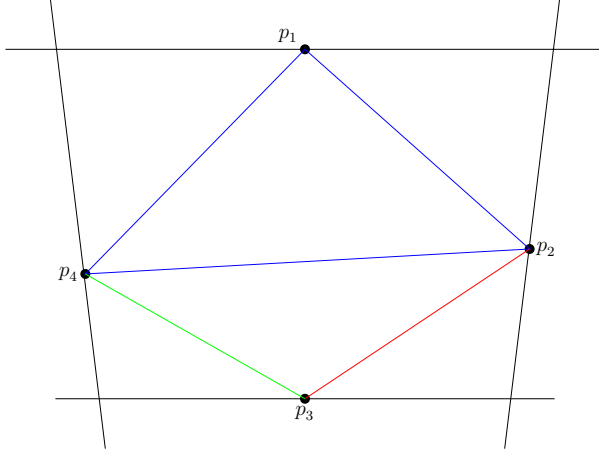


Figure 2.7: Nested triangles in \mathcal{F}_3^+ .

- 2) Now take $F \in \mathcal{F}_4$.


 Figure 2.8: Nested triangles in \mathcal{F}_4^+ .

Given a nested pair of polygons it is easy to compute that $F \in \mathcal{F}_4^+$. So assume $F = (F_1, F_2, F_3, F_4) \in \mathcal{F}_4^+$ and consider the notation from the image on the left. Since $T(F_1, F_2, F_4) > 0$ the blue triangle (p_1, p_2, p_4) is inscribed into (l_1, l_2, l_4) . Because $T(F_1, F_3, F_4) > 0$ and $T(F_1, F_2, F_3) > 0$ the green and red line intersect in a point which lies in the same triangle defined by (l_1, l_2, l_4) as (F_1, F_2, F_4) (the triangles need to be suitably nested).

Finally, because $T(F_2, F_3, F_4) > 0$ the line l_3 does not intersect with the triangle (F_1, F_2, F_4) and the case is proved. Note that:

- 1) that in the image it is also possible for p_3 to lie in the triangle left of $\overline{p_1 p_4}$ or right of $\overline{p_1 p_2}$. The same arguments hold. Observe that the polygon may look different.
- 2) it is easy to see that the product of the four triple ratios above is 1. So the last argument is not necessary but perhaps provides a better understanding.
- 3) The above ideas generalize to arbitrary n , and we will omit the proof here.

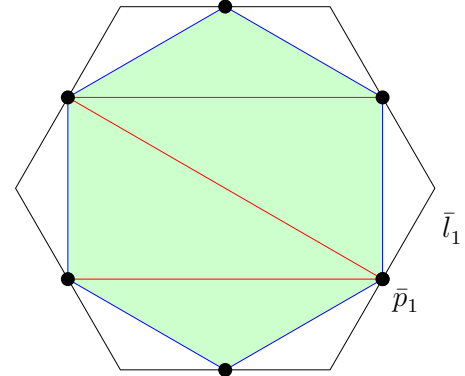
□

To define the parametrization of \mathcal{F}_n^+ we need to introduce some variables.

Let $F = (N, N') = ((\bar{p}_1, \bar{l}_1), \dots, (\bar{p}_n, \bar{l}_n)) \in \mathcal{F}_n^+$ be a pair of suitably nested polygons with a triangulation \mathcal{T} of N such that the vertices of the triangulation are the set of vertices of N , $\{\bar{p}_1, \dots, \bar{p}_n\}$.

Let $I_{\mathcal{T}}$ be the set of internal edges of \mathcal{T} and $\Theta_{\mathcal{T}}$ be the set of triangles of \mathcal{T} .

Note that this triangulation induces a triangulation of a labelled n -gon of M for every $(M, M') \in \mathcal{F}_n^+$.


 Figure 2.9: N' (black), N (blue), $I_{\mathcal{T}}$ (red) and $\Theta_{\mathcal{T}}$ (green).

Now choose $i, j \in \{1, \dots, n\}$ so that \bar{p}_i, \bar{p}_j are endpoints of some internal edge $a_{i,j} \in I_{\mathcal{T}}$. Then let $k, k' \in \{1, \dots, n\}$ so that $i < k < j < k' < i$ in the obvious cyclic ordering on $\{1, \dots, n\}$ and $\bar{p}_i, \bar{p}_j, \bar{p}_k$ and $\bar{p}_i, \bar{p}_j, \bar{p}_{k'}$ are the vertices of the two triangles in $\Theta_{\mathcal{T}}$ that have $a_{i,j}$ as a common edge.

For any $F = ((p_1, l_1), \dots, (p_n, l_n)) \in \mathcal{F}_n^+$ we define

$$\sigma_{i,j}(F) := \log \left(-C(l_i, p_k, p_{k'}, \overline{p_i p_j}) \right)$$

where $\overline{p_i p_j}$ is the projective line through p_i and p_j and C is the cross ratio. From the definition of the cross ratio we can easily see the following lemma which tells us that $\sigma_{i,j}$ is well defined.

Lemma 2.12. For any $(l_1, l_2, l_3, l_4) \in \mathcal{L}_4$ we have $C(l_1, l_2, l_3, l_4) < 0$ if and only if $p_2 \in l_2 \setminus \{p\}$ and $p_3 \in l_3 \setminus \{p\}$ lie in distinct components of $\mathbb{R}P^2 \setminus (l_1 \cup l_4)$.

Proof. From the definition of the cross ratio we see directly that $sign(C)$ is the product of the signs of the four $l_i(p_j)$. Since two lines in $\mathbb{R}P^2$ cut the space only in two connected components the claim follows from a short combinatorial argument. \square

Similarly for $i < j < k < i$ such that there is a triangle $T_{i,j,k} \in \Theta_{\mathcal{T}}$ with vertices $\bar{p}_i, \bar{p}_j, \bar{p}_k$ we define

$$\tau_{i,j,k}(F) := \log T((p_i, l_i), (p_j, l_j), (p_k, l_k))$$

Now if we consider all together we get for every $a_{i,j} \in I_{\mathcal{T}}$ two maps $\sigma_{i,j}, \sigma_{j,i}$ and for every $T_{i,j,k} \in \Theta_{\mathcal{T}}$ one map $\tau_{i,j,k}$. We observe that they are all invariant under $PGL(3, \mathbb{R})$ and thus descend to maps $PGL(3, \mathbb{R}) \setminus \mathcal{F}_n^+ \rightarrow \mathbb{R}$. The following result will end this section and give a parametrization for \mathcal{F}_n^+ .

Proposition 2.13. Let $m = 2 \cdot \#I_{\mathcal{T}} + \#\Theta_{\mathcal{T}}$. The map

$$\left((\sigma_{i,j}, \sigma_{j,i})_{a_{i,j} \in I_{\mathcal{T}}}, (\tau_{i,j,k})_{T_{i,j,k} \in \Theta_{\mathcal{T}}} \right) : PGL(3, \mathbb{R}) \setminus \mathcal{F}_n^+ \rightarrow \mathbb{R}^m$$

is a homeomorphism.

Proof. Denote $\left((\sigma_{i,j}, \sigma_{j,i})_{a_{i,j} \in I_{\mathcal{T}}}, (\tau_{i,j,k})_{T_{i,j,k} \in \Theta_{\mathcal{T}}} \right)$ by $f(F) : PGL(3, \mathbb{R}) \setminus \mathcal{F}_n^+ \rightarrow \mathbb{R}^{2I_{\mathcal{T}} + \Theta_{\mathcal{T}}}$.

It is clear that f is surjective and continuous. For the injectivity consider an argument analogue to the proof of proposition 2.11. Consider $F = (F_1, F_2, F_3, F_4) \in \mathcal{F}_4^+$ with triangulation \mathcal{T} like in the picture. Then $I_{\mathcal{T}} = \{a_{1,3}\}$ and $\Theta_{\mathcal{T}} = \{(F_1, F_2, F_3), (F_3, F_4, F_1)\}$.

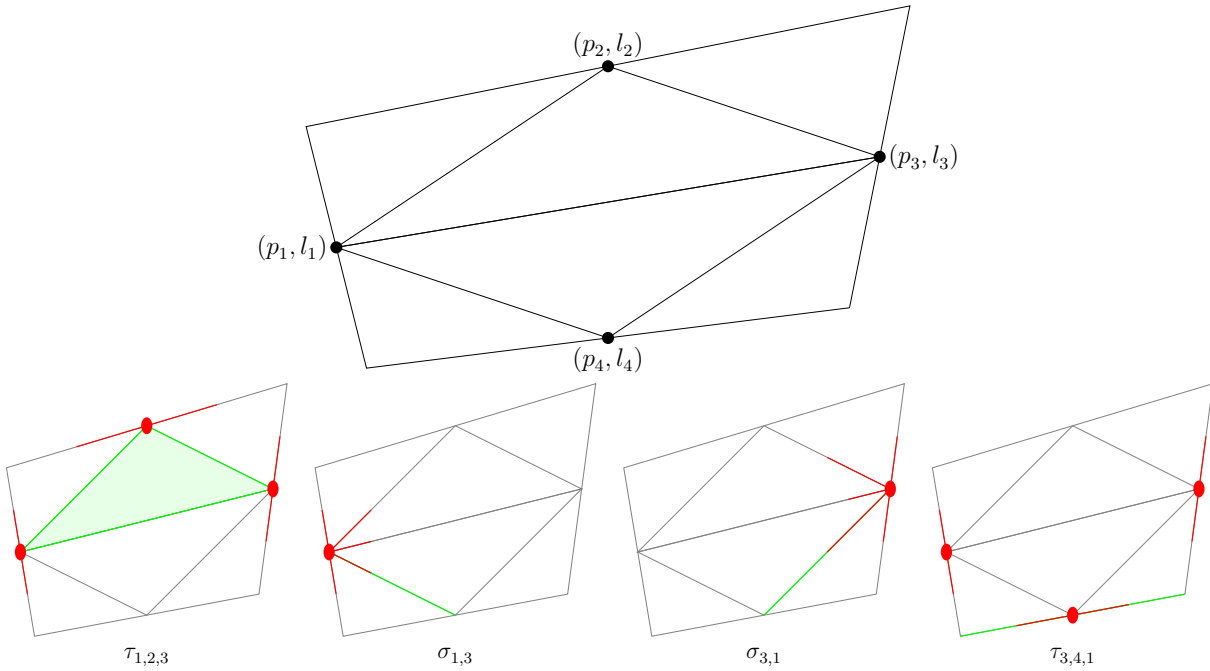


Figure 2.10: Parameters of \mathcal{F}_4^+ . Red marks newly used information and green the resulting information. Read from left to right.

The first triple ratio defines one of the triangles up to $\mathrm{PGL}(3, \mathbb{R})$. Then the point p_4 is determined uniquely (up to $\mathrm{PGL}(3, \mathbb{R})$) by $\sigma_{1,3}$ and $\sigma_{3,1}$ and the line l_4 is determined by the second triple ratio. These observations also generalize directly to \mathcal{F}_n^+ and thus all elements with identical coordinates are equivalent up to $\mathrm{PGL}(3, \mathbb{R})$ in \mathcal{F}_n^+ .

Thus it remains to show that f^{-1} is continuous. This part will be left to the reader. For an idea of the proof see [WZ18] or [FG07]. \square

3 Properly convex sets in \mathbb{RP}^2

In this chapter we construct properly convex sets in \mathbb{RP}^2 . Since we are greatly interested in visualizing these sets and understanding their deformations later on we will start by constructing convex subsets of \mathbb{RP}^2 as the orbit of a group of projective reflections.

As a first approach we investigate the necessary and sufficient conditions to tile convex parts of the sphere and then apply them to generate convex sets as the orbit of a triangle reflection group.

As a second approach we construct convex sets as the orbit of reflection groups generated from suitably nested polygons of n-tuples of flags.

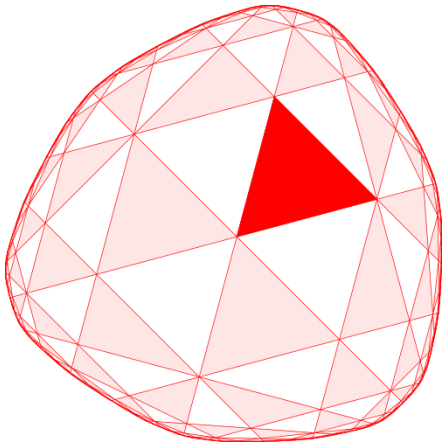


Figure 3.1: Tiling generated by a (3,3,4) triangle group

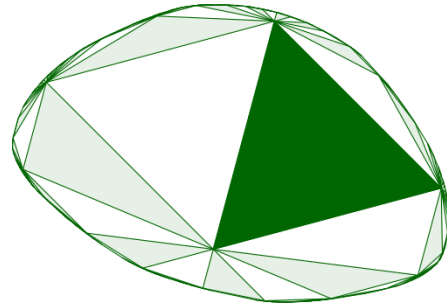


Figure 3.2: Tiling generated by a (5,7,9) triangle group

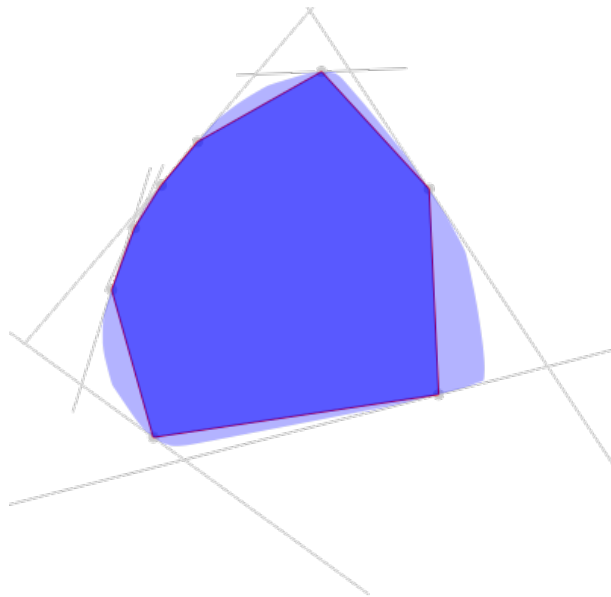


Figure 3.3: Convex set created from eight flags.

We will follow the articles from Benoist [Ben09] and Casselmann [Cas15] for the construction of the convex set Ω via triangle reflection groups and [WZ18] for the approach using flags.

3.1 Tilings of \mathbb{S}^n

Tilings of the euclidian space \mathbb{R}^2 or the hyperbolic plane \mathbb{H}^2 by triangles with angle-sum of the interior angles less or equal to π are well known mathematical visualization. Especially the hyperbolic case is interesting since \mathbb{RP}^2 can be embedded into the projective plane using the Klein Disk model. The interesting fact here is that such tilings now produce, by a suitable choice of reflections, a convex set which is not any more a disk. For this reason we start by considering tilings of convex sets in \mathbb{S}^2 from which we get some nice convex \mathbb{RP}^2 sets later on.

Thus, first we have to define some basic transformations in the projective sphere.

Definition 3.1.1. Let $V = \mathbb{R}^{n+1}$. Then we define the **(projective) sphere** as $\mathbb{S}^n := (V \setminus \{0\})/\mathbb{R}_+^\times$ and its projective transformations $\mathrm{SL}_{n+1}^\pm := \{A \in \mathrm{SL}(n+1, \mathbb{R}) \mid \det(A) = \pm 1\}$.

Definition 3.1.2. A **reflection** in \mathbb{S}^n is an element of order 2 in SL_{n+1}^\pm which is the identity on a hyperplane (in V).

Lemma 3.1. Every reflection R can be written as $R_{\alpha,v} = \mathrm{Id} - \alpha \otimes v$ for $\alpha \in V^*$, $v \in V$ and $\alpha(v) = 2$, e.g. $R(x) = x - \alpha(x)v$.

Proof. First we see that any map $R_{\alpha,v}$ is the identity on $\ker(\alpha)$ and is of order two. So consider a reflection $R \neq \mathrm{Id}$. Without loss of generality R fixes e_{n+1}^\perp and choose $\alpha = (0 \dots 0 \ 1)$. Because R is of order two the last eigenvalue must be -1 with a one dimensional eigenspace E . Choose $v \in E$ such that $v_{n+1} = 2$. Then $R = R_{\alpha,v}$. \square

Definition 3.1.3. A **rotation** in \mathbb{S}^n is an element which is the identity on a subspace of codimension 2 and is given by $\begin{pmatrix} \cos(\theta) & -\sin(\theta) \\ \sin(\theta) & \cos(\theta) \end{pmatrix}$ on the 2-dimensional subspace and in a suitable basis. The **angle of rotation** is θ .

Definition 3.1.4. Let G be a group of reflections and L a closed subset of \mathbb{S}^n . We say (G, L) **tiles** a subset C of \mathbb{S}^n if the interiors $\mathrm{int}(g(L))$, $g \in G$ are disjoint and $C = \bigcup_{g \in G} g(L)$.

We are interested in cases where, for example, triangles tile \mathbb{S}^n or some subset of it. For this we consider two reflections $R_1 = R_{\alpha_1, v_1}$, $R_2 = R_{\alpha_2, v_2}$ and the set

$$L := \{x \in \mathbb{S}^n \mid \alpha_1(x) \leq 0, \alpha_2(x) \leq 0\}.$$

Furthermore, let $a_{12} = \alpha_1(v_2)$ and $a_{21} = \alpha_2(v_1)$. Let G be the group generated by R_1 and R_2 . Let us make a short observation:

Lemma 3.2. If either α_1, α_2 or v_1, v_2 are linearly dependent, then $a_{12}a_{21} = 4$.

Proof. Consider the matrix

$$C = \begin{pmatrix} \alpha_1(v_1) & \alpha_1(v_2) \\ \alpha_2(v_1) & \alpha_2(v_2) \end{pmatrix} = \begin{pmatrix} 2 & a_{12} \\ a_{21} & 2 \end{pmatrix}.$$

If one of the pairs is linearly dependent this matrix is singular. Since

$$0 = \det(C) = 4 - a_{12}a_{21}$$

the result follows. □

Note that in our cases α_1, α_2 are always independent, but we state it in a general setting. It turns out that the values a_{12}, a_{21} are the key to classifying which groups tile the sphere. The following lemma will be the basis for constructing convex domains and tilings later on. Because our main use of this lemma will lie in part b) and c) we will not prove everything in detail here. For further information see [Cas15].

Lemma 3.3. *Using the notation above:*

if $a_{12} > 0$ or $a_{21} > 0$ then (G, L) doesn't tile any subset of \mathbb{S}^n . For $a_{12} \leq 0$ and $a_{21} \leq 0$ we consider

a) $a_{12}a_{21} = 0$: we have either

i) $a_{12} = 0 = a_{21}$: here $G = \mathbb{Z}/2 \times \mathbb{Z}/2$ and (G, L) tiles \mathbb{S}^n

ii) or (G, L) does not tile any subset of \mathbb{S}^n

b) $0 < a_{12}a_{21} < 4$: define θ by $4 \cos^2(\theta/2) = a_{12}a_{21}$. Then R_1R_2 is a rotation of angle θ . If $\theta = \frac{2\pi}{m}$ for $m \geq 3$, then R_1R_2 is of order m and $G = \mathbb{Z}/m \rtimes \mathbb{Z}/2$. In that case (G, L) tiles \mathbb{S}^n . Otherwise not.

c) $a_{12}a_{21} = 4$: then R_1R_2 is unipotent, i.e. all eigenvalues are 1, and (G, L) tiles a subset of \mathbb{S}^n whose closure is a half sphere.

d) $a_{12}a_{21} > 4$: then R_1R_2 has two distinct eigenvalues and (G, L) tiles a subset of \mathbb{S}^n whose closure is the intersection of two half spheres.

Proof. Since each reflection fixes a hyperplane it suffices to consider the case $n = 2$.

We begin with the case $a_{12} > 0$ or $a_{21} > 0$:

Without loss of generality let $a_{12} > 0$. We have for $x \in \text{int}(L)$

$$R_2(x) = R_1(R_2(x)) \Leftrightarrow \alpha_1(x)v_1 = \alpha_1(v_2)\alpha_2(x)v_1 \Leftrightarrow \frac{\alpha_1(x)}{\alpha_2(x)}v_1 = \alpha_1(v_2)v_1$$

The two boundary points of L suffice $\alpha_i(x) = 0$ and $\alpha_j(x) < 0$ for $i \neq j, i, j \in \{1, 2\}$ so

$$\frac{\alpha_1(x)}{\alpha_2(x)} \in (0, \infty), x \in \text{int}(L).$$

The mean value theorem tells us that if $a_{12} > 0$ there is $x \in \text{int}(L)$ such that $R_2(x) = R_1(R_2(x))$. Since reflections send boundary points to boundary points we get

$$R_2(x) \in \text{int}(R_2(L)) \cap \text{int}(R_1(R_2(L))) \neq \emptyset$$

Now we assume $a_{12} \leq 0$ and $a_{21} \leq 0$ for the rest of the proof.

a) A direct computation shows that $R_1R_2 = R_2R_1$ so $G = \mathbb{Z}/2 \times \mathbb{Z}/2$ and the computation above shows that $a_{12} = 0$ implies that $R_2(x) = R_1(R_2(x))$ if and only if $\alpha_1(x) = 0$. This concludes i) since we tile \mathbb{S}^n into 4 regions $L, R_1(L), R_2(L), R_1R_2(L)$.

For ii) one can compute that G fixes a line and tiles each side of the line separately. Thus, (G, L) does not tile a subset of \mathbb{S}^n . For details in this case consider [Cas15, p.7-8].

b) Since this is one of our most important cases we will consider it in more detail below.

c) in this case we have four possibilities for $\alpha_1, \alpha_2, v_1, v_2$ to be linearly (in-)dependent but will only consider the case where both α_1, α_2 and v_1, v_2 are independent. We will start by considering the case in \mathbb{R}^3 . If we consider the reflections in \mathbb{R}^3 and set L to be the intersection of the kernels of the α_i then in the quotient \mathbb{R}^3/L the vectors v_1 and v_2 are linearly dependent.

It is easily shown by a short computation that the reflections become shears along the line through these points. Furthermore, on the line through v_1, v_2 the reflection is a simply multiplication by -1 . A fundamental domain is thus given by the area between the two kernels on one side of that v_1, v_2 -axis.

Considering the action now in n dimensions again, using the fact that $v_1 - v_2$ lies in L we can deduce that the action of G tiles a domain of \mathbb{S}^n whose closure is a half space.

d) This is left to the interested reader.

□

For the proof of b) we have to consider some steps. Again we note that it is sufficient to consider reflections in \mathbb{R}^2 . Let H_1, H_2 be the hyperplanes fixed by R_1 or R_2 , respectively. Then $H_1 \cap H_2$ has codimension 2 and we can consider $\mathbb{S}^2 \subset \mathbb{R}^3$. Choose $x \in H_1 \cap H_2$ as one basis vector and choose the projections of v_1 and v_2 on $(H_1 \cap H_2)^\perp$ for the other two. Then the x -dimension is also fixed, and we have reflections in \mathbb{R}^2 .

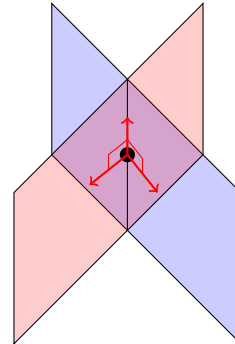


Figure 3.4: Intersecting hyperplanes with basis

For simplicity we use the notation:

$$R_1 = R_{\alpha,v} = \text{Id} - \alpha \otimes v$$

$$R_2 = R_{\beta,w} = \text{Id} - \beta \otimes w$$

Then (v, w) is a basis of \mathbb{R}^2 (since $a_{12}a_{21} \neq 4$).

Next we want to show that R_1R_2 is a rotation, and so we need a suitable basis. Therefore we first see that we can choose $a_{12} = a_{21}$ since scaling, for example $(\alpha, v) \rightarrow (c\alpha, c^{-1}v)$ with $c \neq 0$, does not change the reflection. So without loss of generality let $a = a_{12} = a_{21}$, then:

Lemma 3.4. *Given $0 < a_{12}a_{21} < 4$ and $a_{12}, a_{21} < 0$ there exists a positiv definite, non degenerate inner product \circ on \mathbb{R}^2 such that the two reflections are orthogonal, i.e. $v \perp \ker \alpha, w \perp \ker \beta$.*

Proof. A short computation shows that

$$\ker \alpha = \langle a_{12}v - 2w \rangle$$

$$\ker \beta = \langle 2v - a_{21}w \rangle$$

So assume we have an inner product \circ with the desired properties. Then it needs to suffice

$$\begin{aligned} (a_{12}v - 2w) \circ v &= 0 & (2v - a_{21}w) \circ w &= 0 \\ \Leftrightarrow 2w \circ v &= a_{12}v \circ v & \Leftrightarrow 2w \circ v &= a_{21}w \circ w \end{aligned}$$

So its matrix representation would be

$$\begin{pmatrix} v \circ v & v \circ w \\ w \circ v & w \circ w \end{pmatrix} = (v \circ w) \begin{pmatrix} 2/a_{12} & 1 \\ 1 & 2/a_{21} \end{pmatrix} = (v \circ w) \begin{pmatrix} 2/a & 1 \\ 1 & 2/a \end{pmatrix}$$

Choosing $v \circ w = \frac{a}{2}$ this becomes

$$\begin{pmatrix} 1 & a/2 \\ a/2 & 1 \end{pmatrix}$$

Now if $0 < a^2 < 4$ this matrix is positive definite and non-degenerate. \square

In this setting we have:

$$\begin{aligned} \alpha &= (2 \ a) & v &= \begin{pmatrix} 1 \\ 0 \end{pmatrix} & \ker \alpha &= \left\{ t \begin{pmatrix} 1 \\ -\frac{2}{a} \end{pmatrix} \mid t \in \mathbb{R} \right\} \\ \beta &= (a \ 2) & w &= \begin{pmatrix} 0 \\ 1 \end{pmatrix} & \ker \beta &= \left\{ t \begin{pmatrix} 1 \\ -\frac{a}{2} \end{pmatrix} \mid t \in \mathbb{R} \right\} \end{aligned}$$

and more importantly if τ is the angle between the two reflection axes then by setting $x = (1, -2/a)^T, y = (1, -a/2)^T$ we have

$$\cos^2(\tau) = \frac{|x \circ y|^2}{(x \circ x)(y \circ y)} = \frac{a^2}{4}$$

and thus R_1R_2 is a rotation of $\theta = 2\tau$ where θ is given by $4 \cos^2(\theta/2) = a_{21}a_{12}$. The rest of b) follows directly from that.

3.2 Convexity

For simplicity we are, in this section, interested in tilings by triangles. Yet to be a bit more general we use Lemma 3.3 and state the following theory for 2-dimensional convex polygons $P \subset \mathbb{S}^2$. For the proofs we refer to [Ben09].

Definition 3.2.1. A **convex polygon** P in \mathbb{S}^2 is the convex hull of $n \geq 3$ points p_i where $p_i \in \partial P$ for all $i = 1, \dots, n$.

An **edge** is a 1-dimensional convex subset which is the intersection of ∂P with a hyperplane in \mathbb{R}^3 .

So now whenever we take a convex polygon P we can consider the set of edges S . For every $s \in S$ we choose a projective reflection $R_s = \text{Id} - \alpha_s \otimes v_s$ that fixes s . Without loss of generality we can assume that $P = \{x \mid \alpha_s(x) \leq 0 \forall s\}$. Now let $a_{s,t} = \alpha_s(v_t)$ and Γ be the group generated by the R_s . If we want the images $\{\gamma(P) \mid \gamma \in \Gamma\}$ to tile some subset of \mathbb{S}^2 then the following is necessary:

For all edges s, t such that $s \cap t$ is a point

1. $a_{s,t} \leq 0$ and $(a_{s,t} = 0 \Leftrightarrow a_{t,s} = 0)$
2. $a_{s,t}a_{t,s} \geq 4$ or $a_{s,t}a_{t,s} = 4 \cos^2\left(\frac{\pi}{m_{s,t}}\right)$ with integer $m_{s,t} \geq 2$

This boils down to the following result by Vinberg, mapped to our case \mathbb{S}^2 :

Theorem 3.5 (Vinberg). *Let P be a convex polygon of \mathbb{S}^2 and, for each edge s of P , let $R_s = \text{Id} - \alpha_s \otimes v_s$ be a projective reflection fixing the face s . Suppose that conditions above are satisfied for every s, t such that $\text{codim}(s \cap t) = 2$. Let Γ be the group generated by the reflections R_s . Then*

- a) *the polyhedra $\gamma(P)$, for $\gamma \in \Gamma$, tile some convex subset C of \mathbb{S}^2 ,*
- b) *the group Γ is discrete in $\text{SL}^\pm(3, \mathbb{R})$.*

3.3 Examples

In the following we visualize some examples. They will, most likely, each span one page. Theorywise this is the case when $a_{i,j}a_{j,i} < 4$. All images will show the orbits of the action of triangle reflection groups together with its boundary. Note that we only draw finite iterations and the boundary is C^1 in the limit (see [Ben60]).

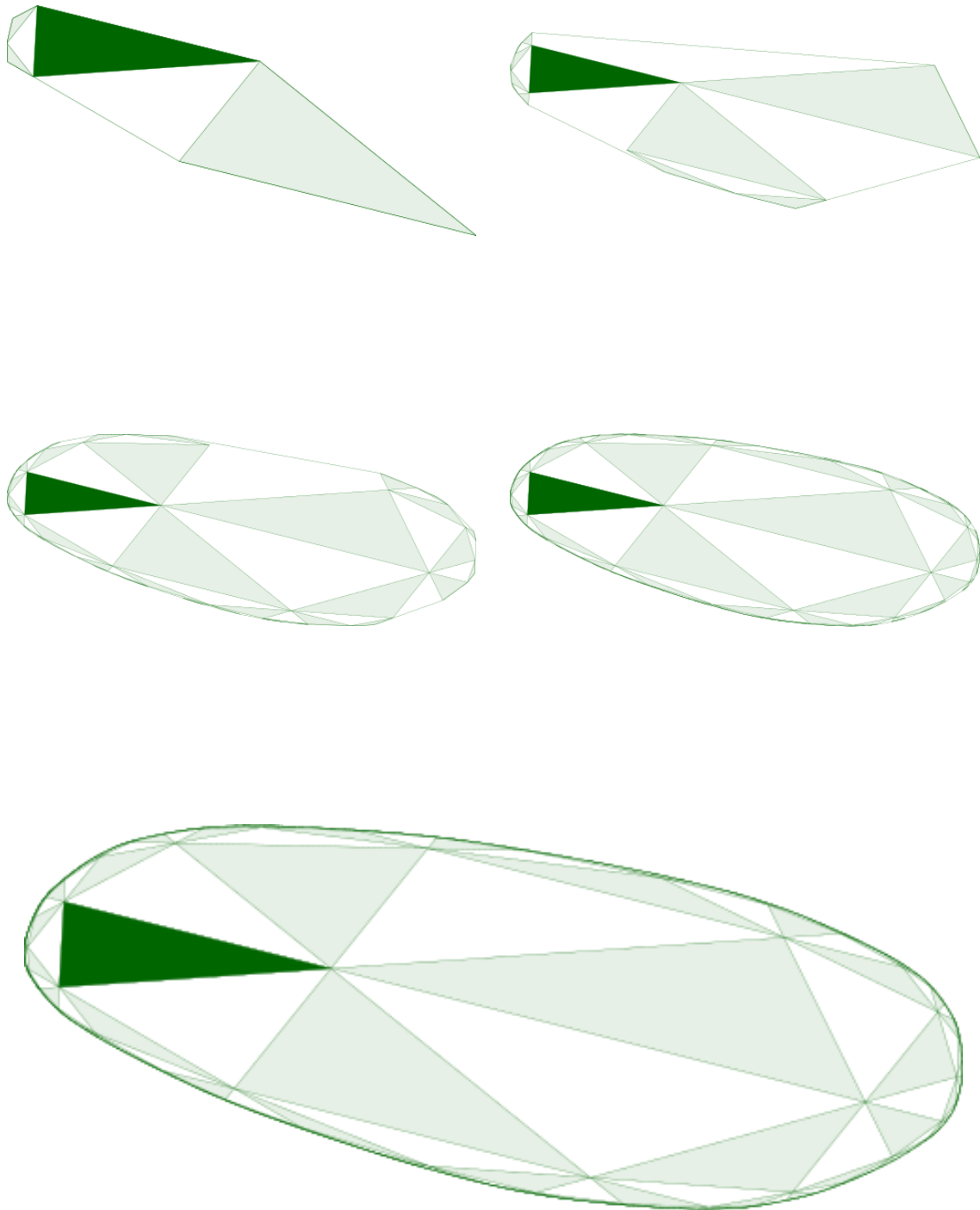


Figure 3.5: Tiling generated by a $(4,4,4)$ triangle reflection group. The depths shown are 1,2,4,6 and 9.

Normal vector for affine plane is $(1, 4, 5)$.

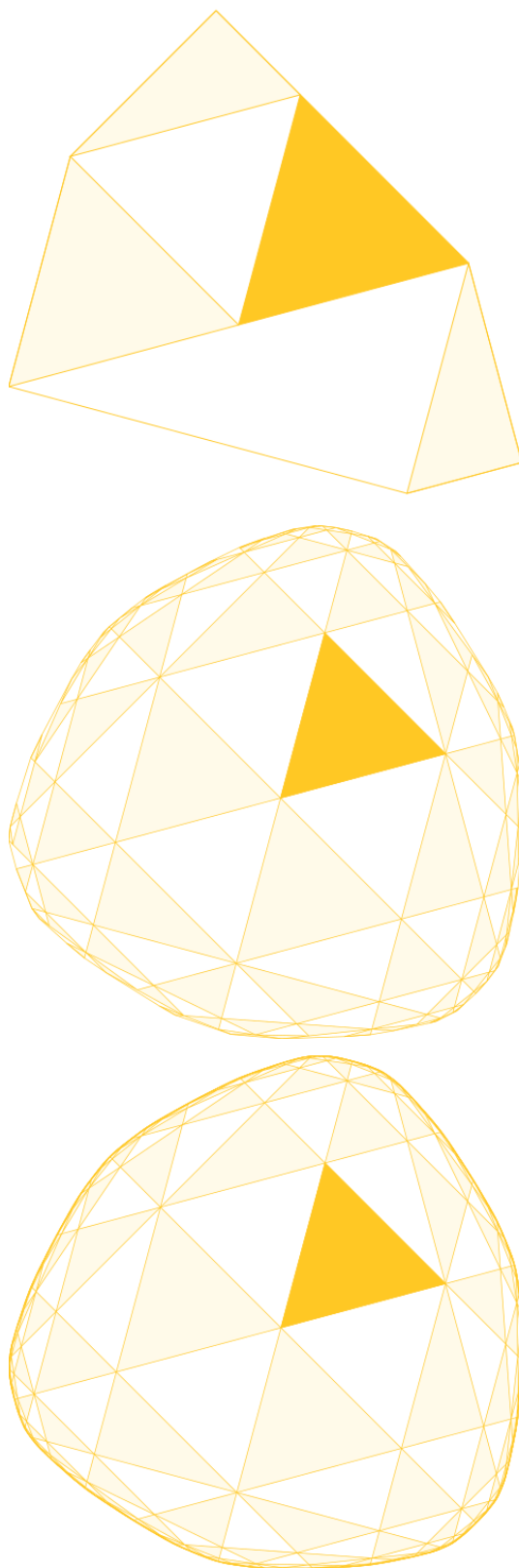


Figure 3.6: Tiling generated by a (3,3,4) triangle group. The depths shown are 1,5 and 10.

Normal vector for affine plane is $(1, 1, 1)$.

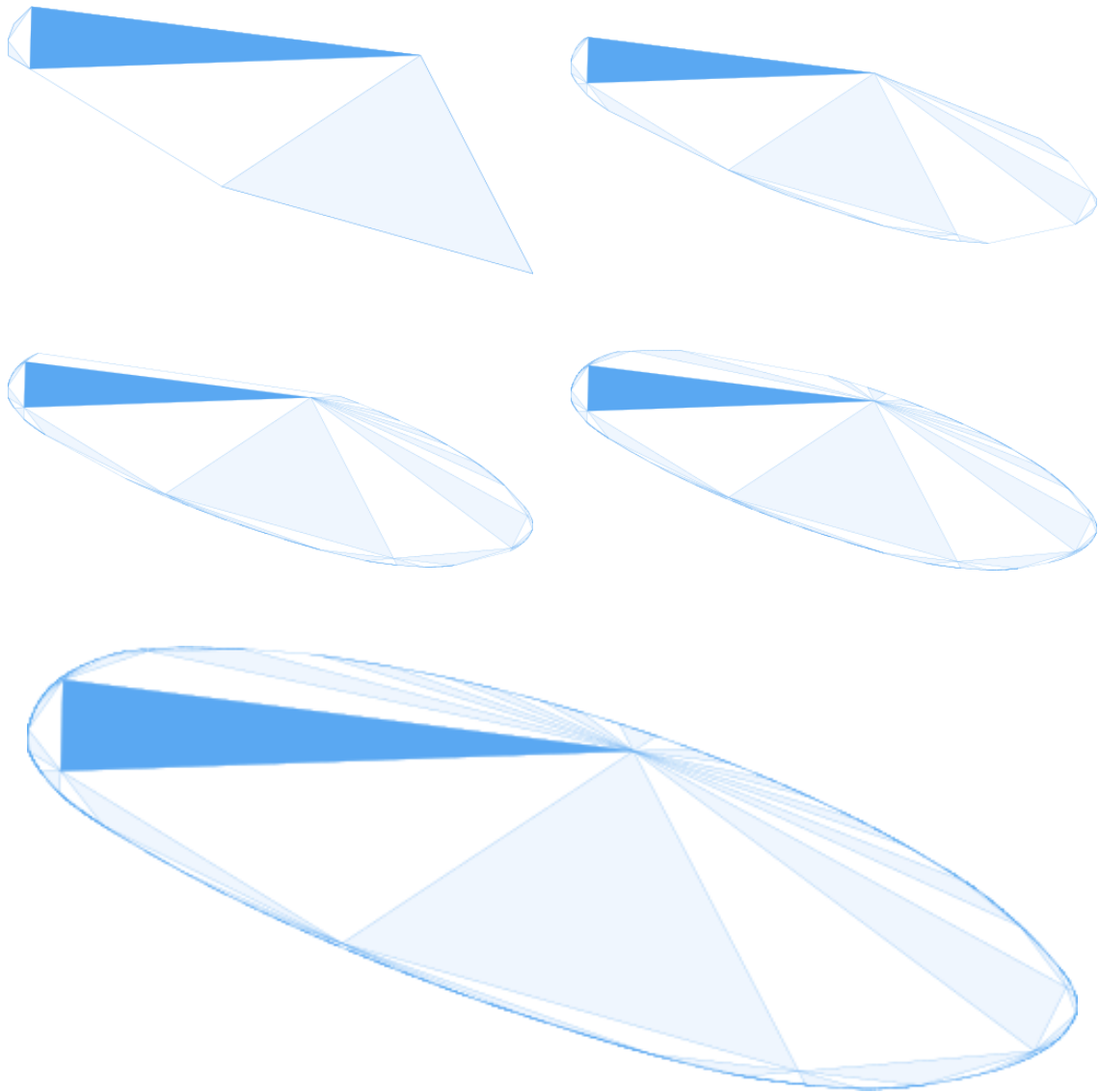


Figure 3.7: Tiling generated by a $(4,8,12)$ triangle group. The depths shown are 1,3,6,8 and 12.
Normal vector for affine plane is $(0.5, 4, 5)$.

3.4 Construction using flags, finite volume polygons

In this section we will use a different approach to construct a properly convex set $\Omega \subset \mathbb{RP}^2$. We will make use of theorem 3.5 of the previous construction. The idea here is that the nested polygon for an element in \mathcal{F}_n^+ creates a tiling of a convex subset inside the outer polygon. Furthermore we will introduce the deformations we are interested in later on tuples of flags. Thus this construction is a solid basis to construct useful convex sets for our purposes. Let $F = (F_1, \dots, F_n) \in \mathcal{F}_n^+$ where $F_i = (p_i, l_i)$ and such that the $(p_i)_i$ are ordered (e.g. clockwise). We obtain two polygons N and N' where N has vertices $(p_i)_i$ and N' has vertices $q_i := l_i \cap l_{i+1}$. Note that the indices are to be taken mod n . We get this picture:

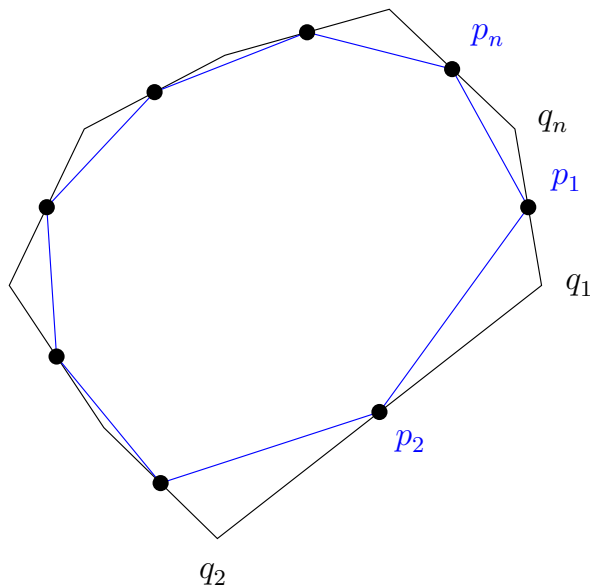


Figure 3.8: N in blue and N' in black.

3.4.1 Construction

First we define the n -gon-reflection group Γ to be the group generated by the reflections along the $(\overline{p_i p_{i+1}})_i$. The reflections are given by

$$R_i := R_{\alpha_i, q_i} = \text{Id} - \alpha_i \otimes q_i$$

with $\alpha_i = \overline{p_i p_{i+1}}$. With this we can define Ω the interior of the union of orbits, i.e.

$$\Omega := \text{int} \left(\bigcup_{\gamma \in \Gamma} \gamma N \right)$$

First of all we want to check if this setting generates a tiling by copies of N . We note here that given two points p, q we have $\overline{pq} = (p \times q)^T$ where \times is the vector crossproduct. Also given two lines $l, k \in \mathbb{RP}^{2*}$ their intersection point can be written as $l \cap k = l^T \times k^T$. Using this and properties of the cross product we get

$$\overline{pq}(l \cap k) = l(p)k(q) - k(p)l(q)$$

It follows

Lemma 3.6. *If $2 = \overline{p_{i-1}p_i}(q_i)$ for all $i = 1, \dots, n$ then we have*

$$\overline{p_{i-1}p_i}(l_{i-1} \cap l_i) \cdot \overline{p_i p_{i+1}}(l_i \cap l_{i+1}) = 4$$

More precisely, whenever two sides of N intersect, e.g. are labelled by consecutive numbers, we have $\alpha_i(q_{i+1})\alpha_{i+1}(q_i) = 4$.

Proof. We know that $2 = \overline{p_{i-1}p_i}(q_i) = \overline{p_{i-1}p_i}(l_{i-1} \cap l_i) = -l_i(p_{i-1})l_{i-1}(p_i)$. Thus using the above formula and $l_i(p_i) = 0$ the result follows. \square

So by theorem 3.5 orbits of N under Γ tile a properly convex subset of \mathbb{S}^n .

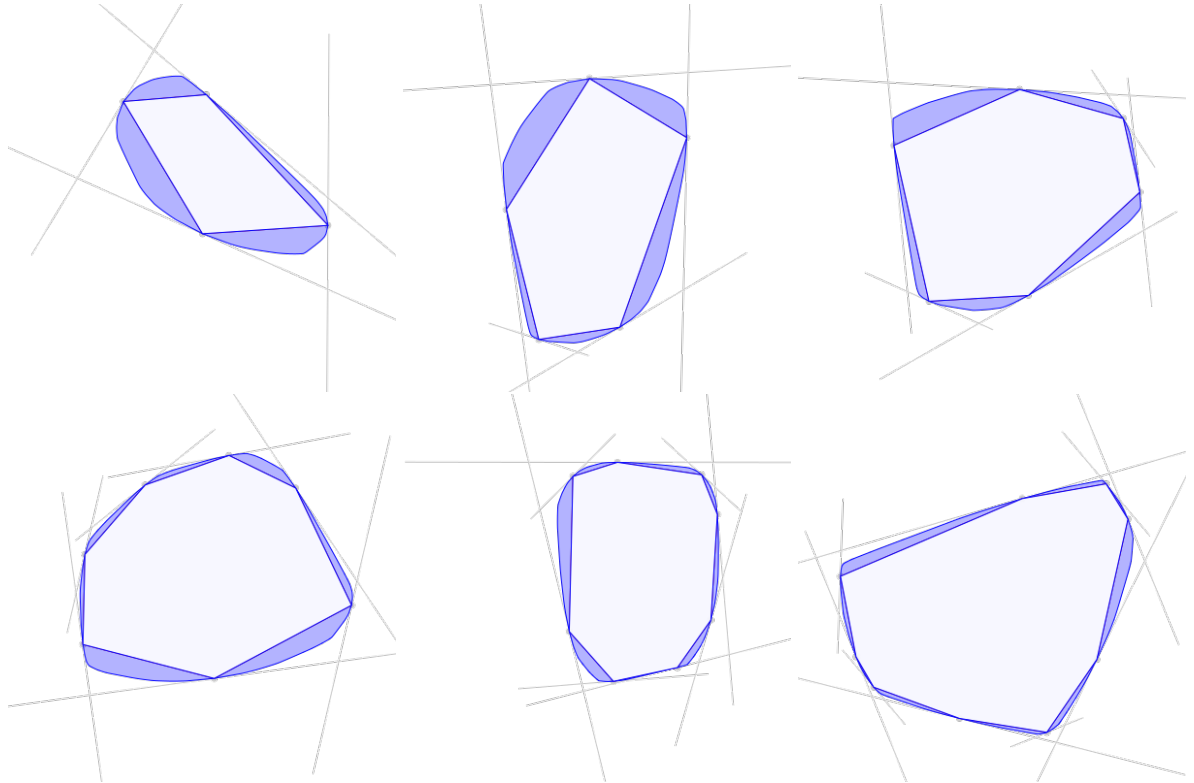


Figure 3.9: Convex sets as boundaries of a union of orbits, drawn with initial n -gon. Shown are values $n = 4, 5, 6, 7, 8, 9$. Flags are drawn in a light gray.

3.4.2 Finite volume

In this subsection we want to draw a connection to hyperbolic cases. We will only sketch the ideas and omit most of the proofs. For more details consider [Mar17].

If we consider an ideal n -gon in \mathbb{H}^2 then it is a well known fact that its hyperbolic area is finite. Note that being ideal simply means that the vertices of our polygon lie on the unit circle, e.g. the boundary of \mathbb{H}^2 .

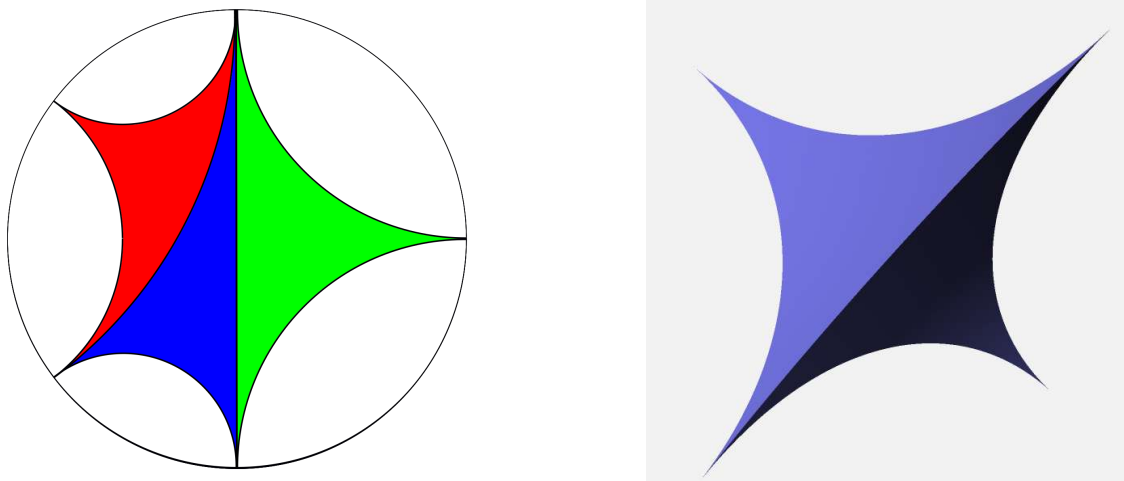


Figure 3.10: Ideal triangles/5-gon in \mathbb{H}^2 and ideal tetrahedron in \mathbb{H}^3 .

If we compare this fact with our construction we see some similarities and this brings up the idea to investigate the volume of the fundamental polygon from which the properly convex set Ω is constructed in the previous subsection. We will understand this connection to hyperbolic geometry in the following part.

On the interior of Ω the Hilbert metric is defined. For any two points $p, q \in \Omega$ let $a, b \in \partial\Omega$ be the points so that a, p, q, b lie on a projective line in \mathbb{RP}^2 in that order. Then

$$d_{\Omega}(p, q) = \frac{1}{2} \log |C(a, p, q, b)|$$

This will define us a so called Finsler metric on Ω which is, after choosing an affine chart and a Euclidean norm, given by

$$F_{\Omega}(x, y) = \frac{|y|}{2} \left(\frac{1}{|xa^{-}|} + \frac{1}{|xa^{+}|} \right)$$

where a^{-} and a^{+} are the intersection points of the half-line starting a in direction $-y$ and y and $|xy|$ is the distance on the affine plane between x and y (see [Ver04]). From this we can define an absolutely continuous measure μ_{Ω} with respect to the Lebesgue measure. We will not need an explicit form for the measure but only state the following:

Proposition 3.7 (stated in [Mar17]). *Let $\Omega_1 \subset \Omega_2$ be two properly convex open sets. Then for any Borel set \mathcal{A} of Ω_1 we have $\mu_{\Omega_2}(\mathcal{A}) \leq \mu_{\Omega_1}(\mathcal{A})$.*

Our goal is the following:

Proposition 3.8. *Let $F = (F_1, \dots, F_n) \in \mathcal{F}_n^+$ and (N, N') be a pair of suitably nested polygons. Let Ω be the convex set constructed like in the last subsection. Then, with regard to the Hilbert metric on Ω , $\mu_{\Omega}(N) < \infty$.*

To prove we follow directly from this lemma:

Lemma 3.9. *Let $F_i = (p_i, l_i)$. Assume that for each $i = 1, \dots, n$ there is an ellipse $E_i \subset \Omega$ such that $\partial E_i \cap \partial\Omega = \{p_i\}$, $p_j \notin E_i$ for $j \neq i$ and $E_i \cap E_j = \emptyset$ has only two connected components. If $\mu_{\Omega}(N \cap E_i) < \infty$ then $\mu_{\Omega}(N) < \infty$.*

Proof. The assumptions allow us to cut N into $n + 1$ components M, M_1, \dots, M_n where $M_i = N \cap E_i$ and $M = N \setminus \bigcup_{i=1, \dots, n} M_n$. In this case M is compact and thus $\mu_\Omega(M) < \infty$. It follows

$$\mu_\Omega(N) = \mu_\Omega(M) + \sum_{i=1}^n \mu_\Omega(M_i) < \infty.$$

This proves the claim. □

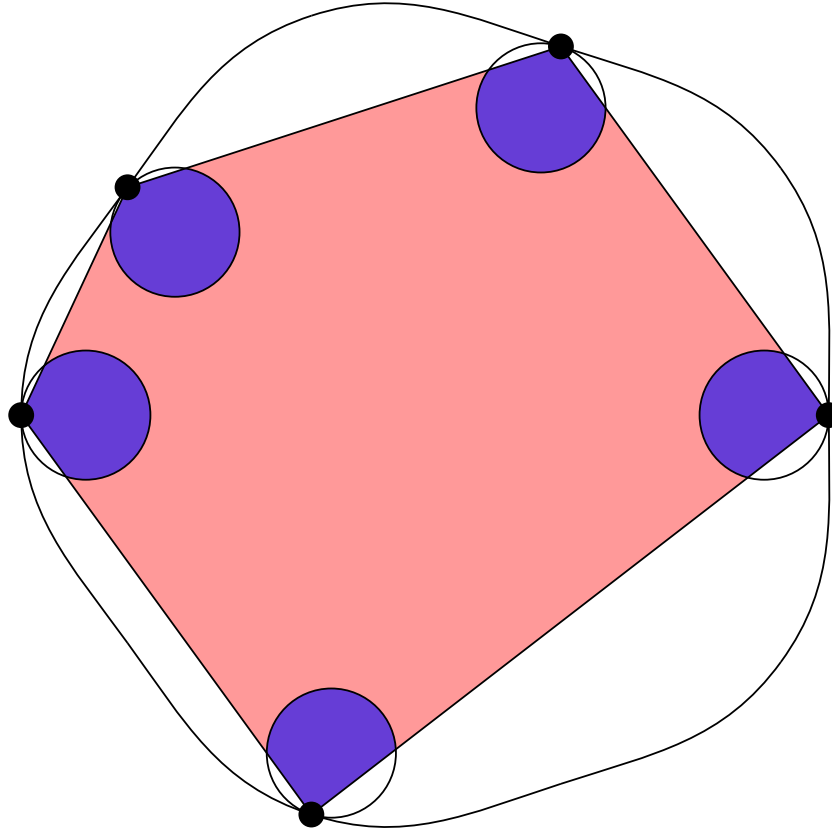


Figure 3.11: Cutting up a suitably nested polygon to compute its volume.

So what we need to show is that we can find these ellipses E_i such that $\mu_\Omega(N \cap E_i) < \infty$. We will from now on only consider the case for a single $i \in \{1, \dots, n\}$ and denote the needed data as p, l, E, N instead of p_i, l_i, E_i, N .

From the construction of Ω we know that the setting is as follows: l is the tangent on Ω at p and we consider two reflections R_1, R_2 along lines α, β with fix point v, w (see figure 3.12 (left)). Because the group action tiles a half space the images under the reflections is given as shown. The next lemma allows us to simplify the problem a little bit.

Lemma 3.10. *For every $t > 0$ there exists a transformation $g \in \text{PGL}(3, \mathbb{R})$ fixing α, β, p and w that sends v to v' where $\text{dist}_{\text{eucl}}(v', p) = t \cdot \text{dist}_{\text{eucl}}(v, p)$.*

Proof. Choose a basis $e_1 = p, e_2 = w, e_3$ where e_3 defines β . By scaling the e_i we can assume that α is defined by $[1, 1, 1]^T$.

Now g fixes α, β, p, w , thus it is given by

$$\begin{bmatrix} \lambda_1 & 0 & \mu_1 \\ 0 & \lambda_2 & 0 \\ 0 & 0 & \mu_2 \end{bmatrix},$$

e.g. $[e_1] \mapsto [\lambda_1 e_1] = [e_1]$ and $[e_3] \mapsto [\mu_1 e_1 + \mu_2 e_3] \in \beta$. Because g fixes α , i.e.

$$[1, 1, 1]^T \mapsto \varepsilon_1 e_1 + \varepsilon_2 [1, 1, 1]^T$$

it follows that $\lambda_2 = \mu_2$. The coordinates of v are given by $[x, y, 0]^T$ and thus $g(v) = [\lambda_1 x, \lambda_2 y, 0]^T$. Since we can choose the scalars arbitrarily $v' = g(v)$ can be chosen as wished.

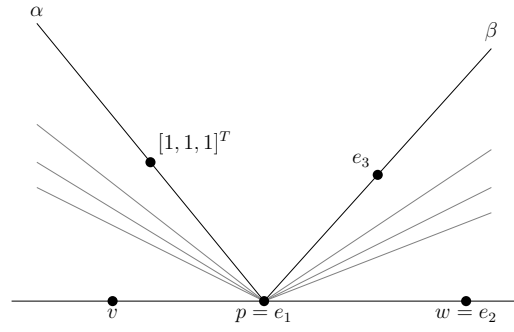


Figure 3.12: Setting around a point p with two reflections.

□

This simply means that we can transform our setting by a map in $\text{PGL}(3, \mathbb{R})$ such that v lies suitably on l . Especially we can choose v in a way that there is a circle S with the following properties:

- i) $S \cap l = \{p\}$,
- ii) there are points $x, y \in S$ such that v, w are the intersections of l with the tangents on S at x and y , respectively

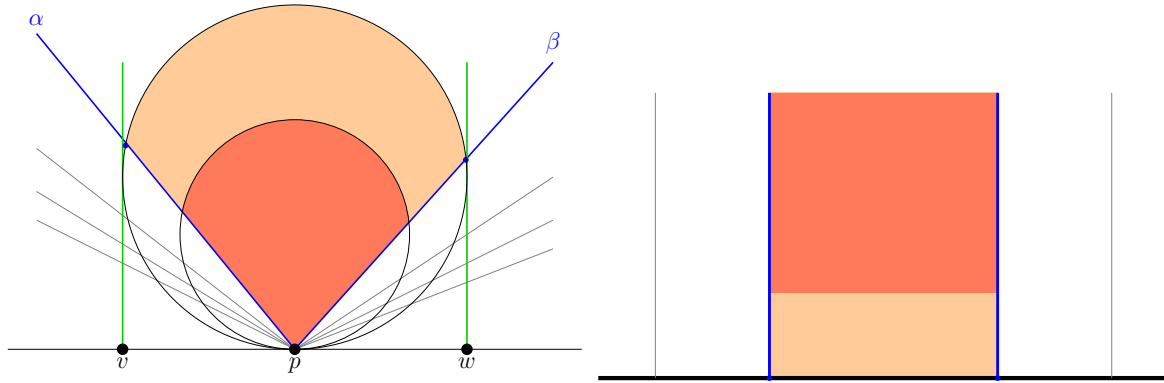


Figure 3.13: The spheres S, S' and $S \cap N, S' \cap N$ shown in orange and red. On the right we have the upper half space model with p being mapped to ∞ .

With this we can use our knowledge from hyperbolic geometry, i.e. S is preserved by the two reflections (that can be seen easily using the upper half plane model, see figure 3.13(right)) and thus S is a subset of the union of orbits of that action. We can now choose a smaller sphere $S' \subset S$ touching p and which is also preserved by the reflections. For any choice of S' we then get $\mu_S(S' \cap N) < \infty$.

Let S^* be the ellipse obtained from S and E the one obtained from S' . Using proposition 3.7 we get from $E \subset S^* \subset \Omega$ that $\mu_\Omega(E \cap N) \leq \mu_{S^*}(E \cap N) < \infty$. Note that projective transformations do not change the measure since they are isometries for the Hilbert metric. This immediately proves proposition 3.8.

3.5 Examples

In the following we will see pictures of two examples. In this case it is not so easy to see the change for each level so we include a more detailed view of each example. Theorywise this is the case when $a_{i,j}a_{j,i} = 4$.

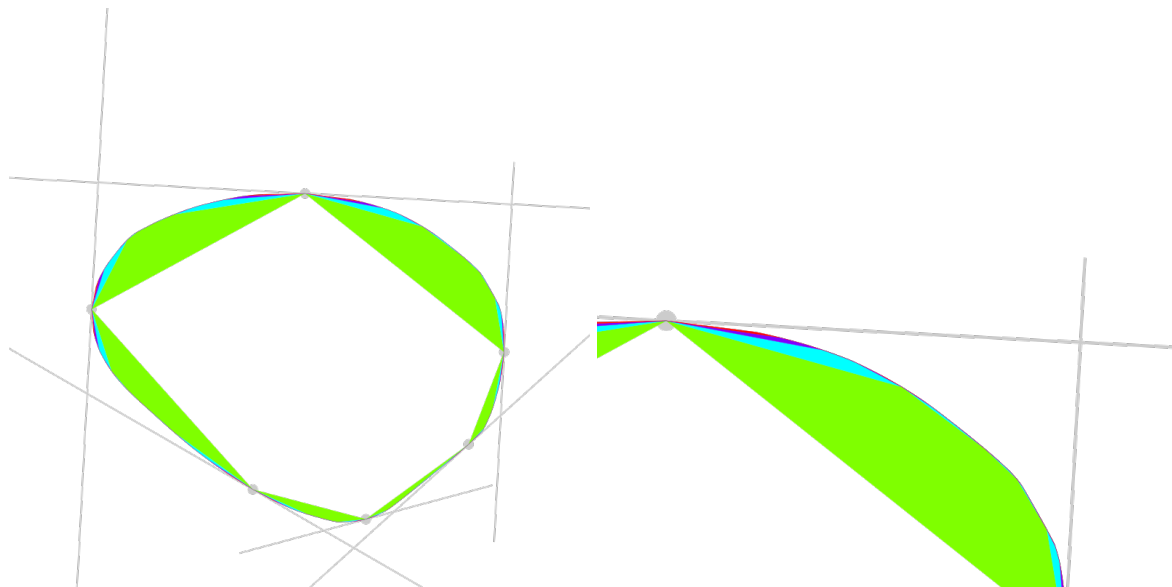


Figure 3.14: Construction of convex set via flags. Each level is differently coloured. This is a 6-gon, 4 levels deep.

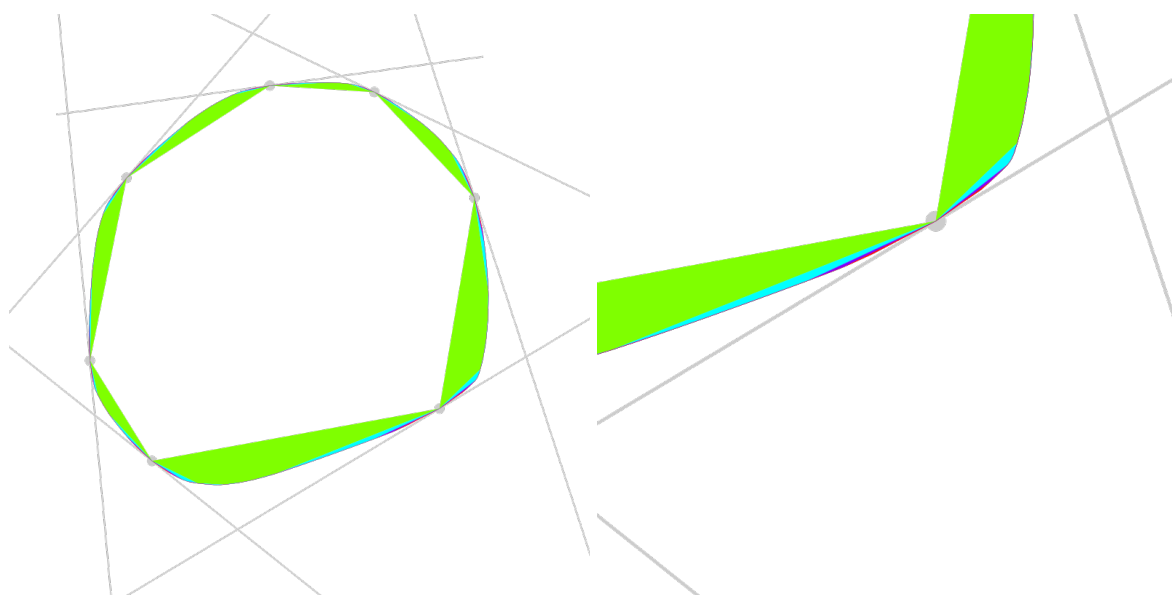


Figure 3.15: Construction of convex set via flags. Each level is differently coloured. This is a 7-gon, 4 levels deep.

4 Deformations of convex sets in \mathbb{RP}^2

In this chapter we want to take a look at some deformations of convex sets in \mathbb{RP}^2 . We will make use of the projective invariant defined previously and define 1-parameter families of transformations that continuously change the invariants. First we take a look at the triple ratio and triples of flags. Their deformation will be described by the eruption flow. Afterwards we take a look at 4-tuples of flags. There, using a division into two triangles we define the bulging and shearing flows to understand the change in the invariants defined by the cross ratio. After considering the generalization on n -tuples of flags we give a short insight into the case of convex sets with C^1 -boundary. There we will discuss how the defined flows can be generalized onto the convex sets with C^1 -boundary by using two approaches and looking at their connection.

4.1 Flag deformations

In this section we want to define deformations of \mathcal{F}_n^+ . Therefore we will start with \mathcal{F}_3^+ and \mathcal{F}_4^+ and generalize these methods to the n -dimensional case.

4.1.1 Triples in \mathcal{F}_3^+

Let $(F_1, F_2, F_3) \in \mathcal{F}_3^+$ and (Δ, Δ') be the corresponding pair of suitably nested labelled triangles. We remember the notation from notation 2.3.3. We first want to obtain three quadrilaterals from (Δ, Δ') . We did this before in figure 2.5:

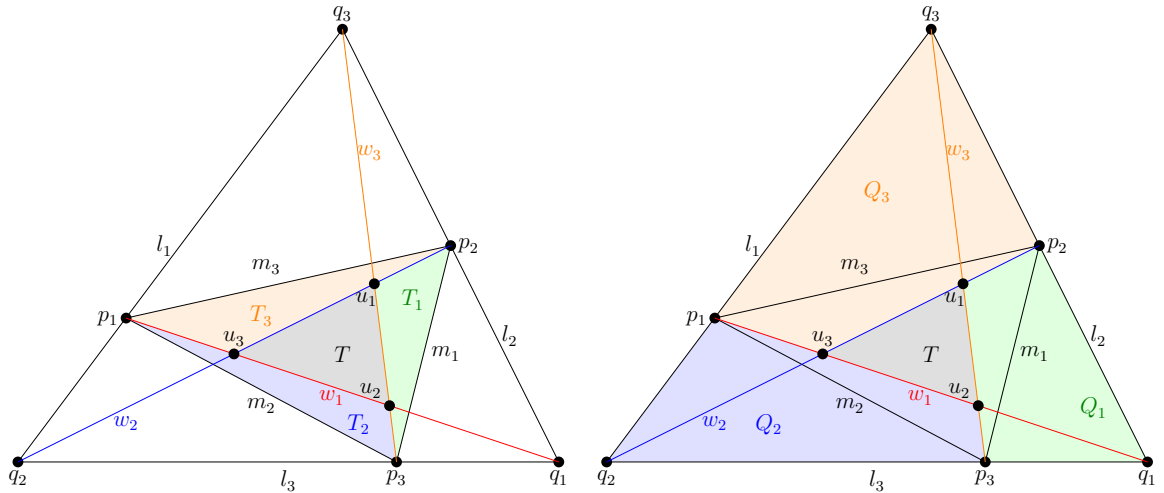


Figure 4.1: Nested triangle in a triple of flags $F \in \mathcal{F}_3^+$ and partition into quadrilaterals plus triangle.

So define

$$\Delta = T \cup T_1 \cup T_2 \cup T_3$$

$$\Delta' = T \cup Q_1 \cup Q_2 \cup Q_3$$

Conversely we can use this and proposition 2.9 to construct a pair of suitably nested triangles from three labelled quadrilaterals in \mathcal{P}_4 as follows:

Up to $\text{PGL}(3, \mathbb{R})$ there is a unique labelled quadrilateral, so we may assume that all quadrilaterals are the same; then using the triple or cross ratio assemble them in the right way. To see an explicit construction see section 5.3.

This also shows that we only need to change or deform those assembly instructions to get a path in $\mathcal{F}_3^+ \setminus \text{PGL}(3, \mathbb{R})$.

To be explicit we choose a basis (q_1, q_2, q_3) (reminder: actually choose v_1, v_2, v_3 representatives) and define the maps

$$g_1(t) = \begin{bmatrix} 1 & 0 & 0 \\ 0 & e^{t/3} & 0 \\ 0 & 0 & e^{-t/3} \end{bmatrix} \quad g_2(t) = \begin{bmatrix} e^{-t/3} & 0 & 0 \\ 0 & 1 & 0 \\ 0 & 0 & e^{t/3} \end{bmatrix} \quad g_3(t) = \begin{bmatrix} e^{t/3} & 0 & 0 \\ 0 & e^{-t/3} & 0 \\ 0 & 0 & 1 \end{bmatrix}$$

Lemma 4.1. *For all $i = 1, 2, 3$ $p' = g_{i-1}(t)(p_i) = g_{i+1}(p_i)$ lies on l_i and $u_i(t) := g_i(t)(u_i)$ lies on the line through q_{i-1} and $g_i(t)(p_{i-1})$.*

Proof. Here it is important to note that we have projective equivalence classes.

The first statement follows directly from the fact that

$$l_i = e_i^T \quad p_1 = \begin{pmatrix} 0 \\ a \\ b \end{pmatrix} \quad p_2 = \begin{pmatrix} c \\ 0 \\ d \end{pmatrix} \quad p_3 = \begin{pmatrix} e \\ f \\ 0 \end{pmatrix}$$

The second statement follows from a simple calculation (see proof of proposition 2.9 for help). □

This implies that we are in a similar setting as above and there is a unique labelled triangle $T(t)$ such that $(\Delta(t), \Delta'(t)) \in \mathcal{F}_3^+$ where

$$\begin{aligned} \Delta'(t) &:= (g_1(t)(Q_1)) \cup (g_2(t)(Q_2)) \cup (g_3(t)(Q_3)) \cup T(t) \\ \Delta(t) &:= (g_1(t)(T_1)) \cup (g_2(t)(T_2)) \cup (g_3(t)(T_3)) \cup T(t) \end{aligned}$$

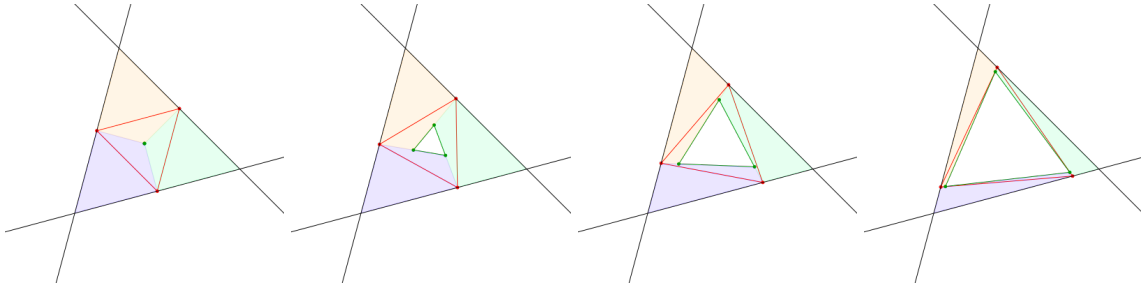


Figure 4.2: Triple of flags with triple ratio 1 and its eruptions for values $t = 1, 2.5, 5$. $\Delta(t)$ in red and $T(t)$ in green.

Definition 4.1.1. The **eruption flow** on \mathcal{F}_3^+ is the flow $\varepsilon_t : \mathcal{F}_3^+ \rightarrow \mathcal{F}_3^+$ defined by $(\Delta, \Delta') \mapsto (\Delta(t), \Delta'(t))$.

Using this flow we can describe the change in the assembly instruction. To be exact:

Proposition 4.2. *Let $(F_1(t), F_2(t), F_3(t)) \in \mathcal{F}_3^+$ be the triple of flags corresponding to $(\Delta(t), \Delta'(t))$. Then*

$$T(F_1(t), F_2(t), F_3(t)) = e^t T(F_1, F_2, F_3)$$

Proof. Choosing the usual setting we get

$$g_3(t)p_1 = \begin{pmatrix} 0 \\ a \cdot e^{-t/3} \\ b \end{pmatrix} \quad g_1(t)p_2 = \begin{pmatrix} c \\ 0 \\ d \cdot e^{-t/3} \end{pmatrix} \quad g_2(t)p_3 = \begin{pmatrix} e \cdot e^{-t/3} \\ f \\ 0 \end{pmatrix}$$

and thus

$$T(F_1(t), F_2(t), F_3(t)) = \frac{cfb}{e^{-t}ade} = e^t T(F_1, F_2, F_3)$$

□

As a last remark regarding \mathcal{F}_3^+ it is nice to note that the name comes from imagining \triangle as a volcano with T being the opening of the volcano. As $t > 0$ grows the opening becomes bigger.

Another nice visualization is the following where t ranges from 0 (red) to $e^{\pm 29}$ (purple) by applying an $t = \pm 0.2$ eruption a hundred times.

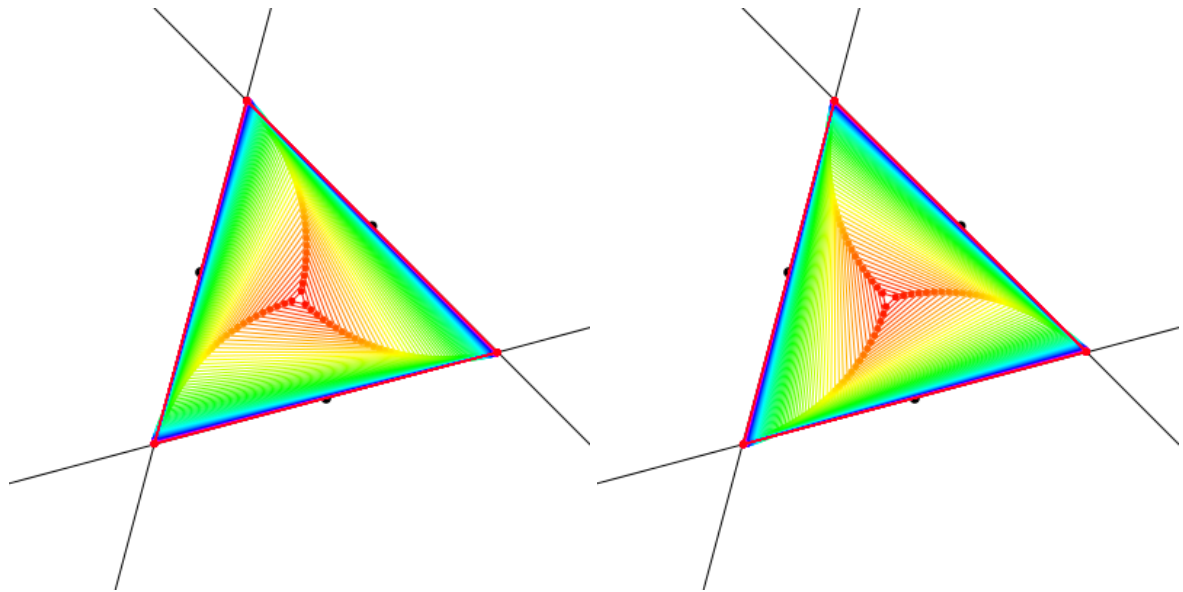


Figure 4.3: Triangle T for triple ratio 1 and erupting a hundred times with $t = 0.2$ (left) or $t = -0.2$ (right).

4.1.2 Quadruples in \mathcal{F}_4^+

Consider a quadruple $(F_1, F_2, F_3, F_4) \in \mathcal{F}_4^+$ with its associated pair of nested quadrilaterals (N, N') . We want to split N into two triangles along an oriented line segment. Let N_L, N_R be the two triangles left and right of that line segment $a_{1,3}$ defined by

$$N_L = (F_1, F_3, F_2) \quad N_R = (F_1, F_3, F_4)$$

We call p_1 the backward point and p_3 the forward point.

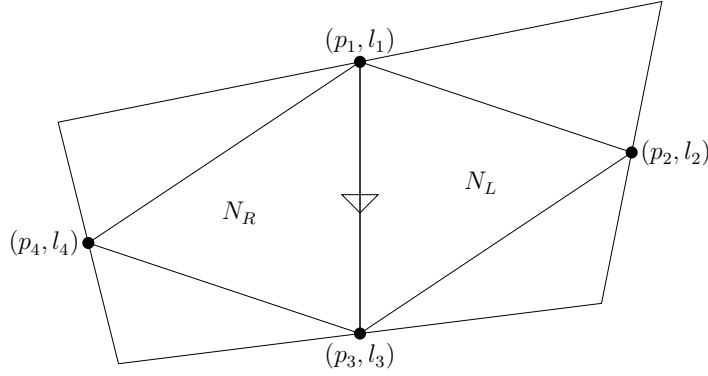


Figure 4.4: Decomposition of $F \in \mathcal{F}_4^+$ into (N, N') with triangulation.

Also $a_{1,3}$ decomposes N' into two quadrilaterals.

We now define deformations associated to the above decomposition of N into two triangles. Let $v_1, v_3, v_{1,3}$ be vectors that span p_1, p_3 and the intersection point $l_1 \cap l_3$. In the basis $(v_1, v_{1,3}, v_3)$ define the following transformations in $\text{PGL}(3, \mathbb{R})$

$$s(t) = \begin{bmatrix} e^{t/2} & 0 & 0 \\ 0 & 1 & 0 \\ 0 & 0 & e^{-t/2} \end{bmatrix} \quad b(t) = \begin{bmatrix} e^{-t/6} & 0 & 0 \\ 0 & e^{t/3} & 0 \\ 0 & 0 & e^{-t/6} \end{bmatrix}$$

Definition 4.1.2. 1) Let

$$\begin{aligned} N(t) &:= (s(t) \cdot N_L) \cup (s(-t) \cdot N_R) \\ N'(t) &:= (s(t) \cdot N'_L) \cup (s(-t) \cdot N'_R) \\ M(t) &:= (b(t) \cdot N_L) \cup (b(-t) \cdot N_R) \\ M'(t) &:= (b(t) \cdot N'_L) \cup (b(-t) \cdot N'_R) \end{aligned}$$

2) The **shearing flow** on \mathcal{F}_4^+ associated to $a_{1,3}$ is the flow

$$(\gamma)_t : \mathcal{F}_4^+ \longrightarrow \mathcal{F}_4^+, (N, N') \mapsto (N(t), N'(t))$$

3) The **bulging flow** on \mathcal{F}_4^+ associated to $a_{1,3}$ is the flow

$$(\beta)_t : \mathcal{F}_4^+ \longrightarrow \mathcal{F}_4^+, (N, N') \mapsto (M(t), M'(t))$$

Lemma 4.3. *The shearing and bulging flows on \mathcal{F}_4^+ are well defined.*

Proof. It is easy to see that $s(t)$ and $b(t)$ both fix p_1 and p_3 . Since the matrices are diagonal in this basis and points on the lines $a_{1,3}, l_1$ or l_3 are given by points where one entry is always zero we see that both flows stabilize the three lines.

Thus $(N(t), N'(t))$ and $(M(t), M'(t))$ are suitably nested, labelled quadrilaterals. \square

As in the case with the eruption flow these flows change the invariants, in this case the cross ratio, in an easy way

Proposition 4.4. *Let $(F_1(t), F_2(t), F_3(t), F_4(t)) \in \mathcal{F}_4^+$ be the quadruple corresponding to $(N(t), N'(t))$. Then, if \overline{xy} is the projective line through x and y ,*

$$\begin{aligned} C(l_1(t), p_2(t), p_4(t), \overline{p_1(t)p_3(t)}) &= e^t C(l_1, p_2, p_4, \overline{p_1 p_3}) \\ C(l_3(t), p_4(t), p_2(t), \overline{p_1(t)p_3(t)}) &= e^t C(l_3, p_4, p_2, \overline{p_1 p_3}) \end{aligned}$$

And if $(F_1(t), F_2(t), F_3(t), F_4(t)) \in \mathcal{F}_4^+$ is the quadruple corresponding to $(M(t), M'(t))$, then

$$\begin{aligned} C(l_1(t), p_2(t), p_4(t), \overline{p_1(t)p_3(t)}) &= e^t C(l_1, p_2, p_4, \overline{p_1 p_3}) \\ C(l_3(t), p_4(t), p_2(t), \overline{p_1(t)p_3(t)}) &= e^{-t} C(l_3, p_4, p_2, \overline{p_1 p_3}) \end{aligned}$$

Proof. Given the basis $(v_1, v_{1,3}, v_3)$ and using figure 4.4 as help we find representatives for the first case $((N(t), N'(t)))$:

$$\begin{aligned} l_1 = l_1(t) &= (0, 0, 1) & p_2 &= (a, b, c) & p_2(t) &= (e^{t/2}a, b, e^{-t/2}c) \\ l_3 = l_3(t) &= (1, 0, 0) & p_4 &= (x, y, z) & p_4(t) &= (e^{-t/2}x, y, e^{t/2}z) \\ L := \overline{p_1 p_3} = \overline{p_1(t)p_3(t)} &= (0, 1, 0) \end{aligned}$$

Thus it is easy to see that

$$\begin{aligned} C(l_1(t), p_2(t), p_4(t), \overline{p_1(t)p_3(t)}) &= \frac{e^{t/2}zb}{e^{-t/2}cy} \\ &= e^t \frac{zb}{cy} = e^t C(l_1, p_2, p_4, \overline{p_1 p_3}) \end{aligned}$$

The rest is proven in the same way. □

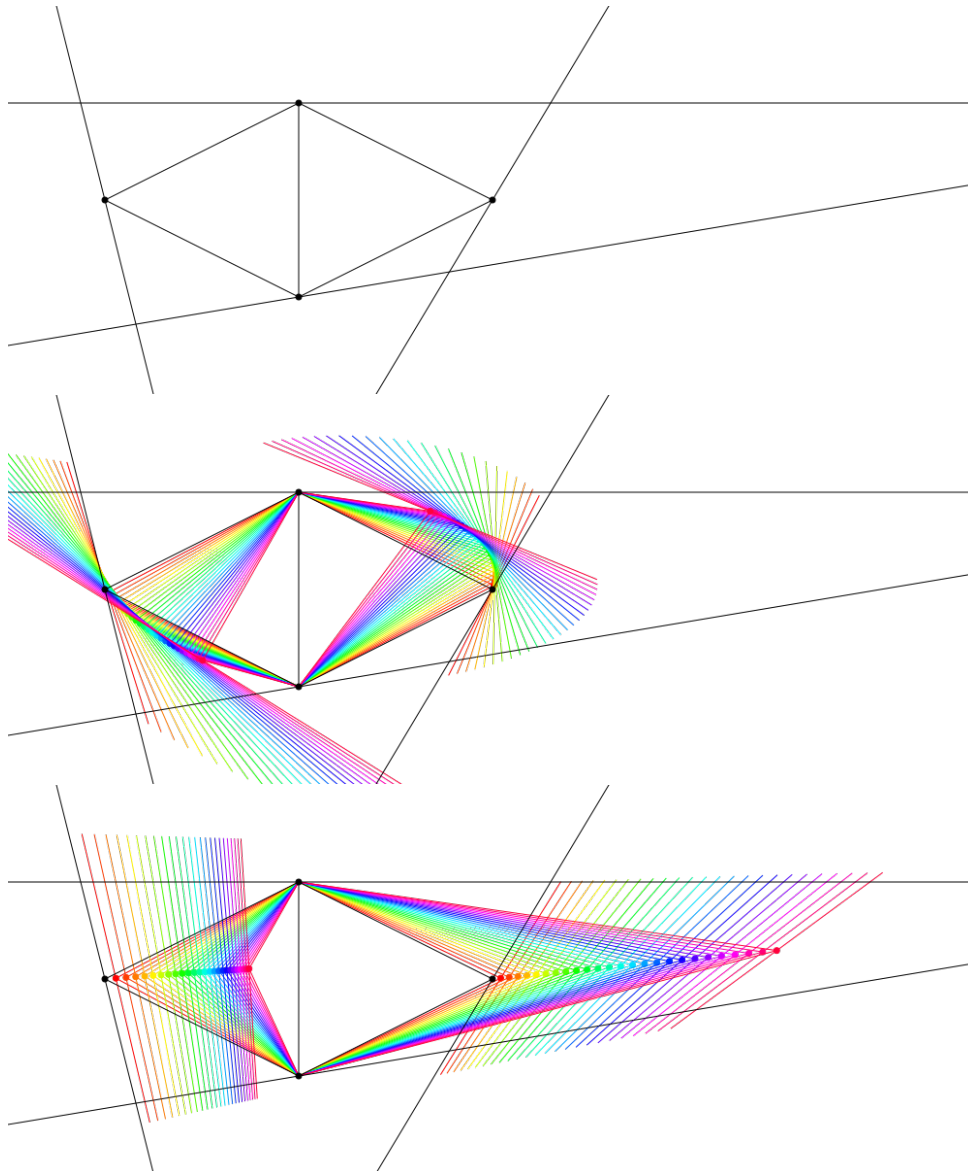


Figure 4.5: Initial $F \in \mathcal{F}_4^+$, shearing deformation and bulging deformation. 25 times deformed with $t = 0.1$ (red over green and purple to red).

Here we draw deformations using shearing and bulging flows on \mathcal{F}_4^+ together

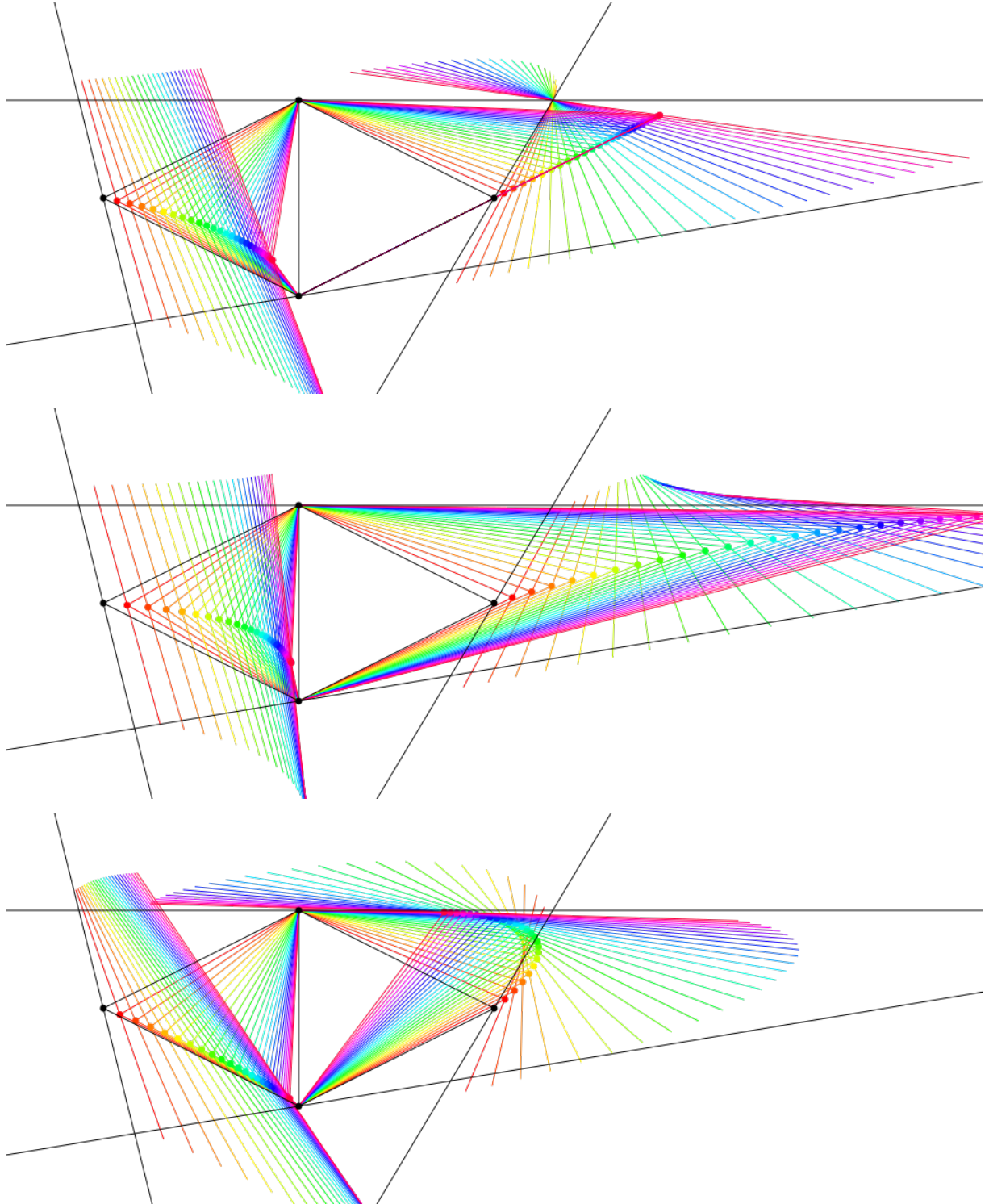


Figure 4.6: Initial $F \in \mathcal{F}_4^+$. First image is shear and bulge in each step with $t = 0.1$. Second is bulge with $t = 0.2$, shear with $t = 0.1$ and third is bulge with $t = 0.1$, shear with $t = 0.2$

4.1.3 n -tuples in \mathcal{F}_n^+

Now we have all the transformations for $n = 3, 4$ and thus we are ready to generalize this. Let $(N, N') = ((p'_1, l'_1), \dots, (p'_n, l'_n)) \in \mathcal{F}_n^+$ and choose a triangulation like in proposition 2.11.

Let $a_{i,j}$ be the edge of the triangulation with endpoints p'_i, p'_j . Since the vertices of N are labelled we get an induced orientation on N and $a_{i,j}$ cuts both N and N' in two labelled polygons. Note that they are always non-empty unless $a_{i,j}$ is a boundary segment of N .

Define the labelled polygons N_L, N_R, N'_L, N'_R such that N_L, N'_L lie on the left side of $a_{i,j}$ and N_R, N'_R lie on the right side, $N_L \cup N_R = N$ and $N'_L \cup N'_R = N'$.

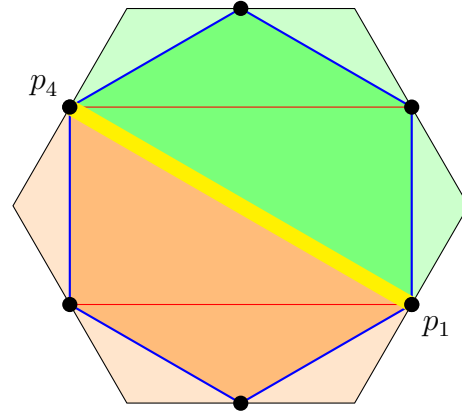


Figure 4.7: N_L, N'_L (orange), N_R, N'_R (green) and $a_{1,4}$ (yellow)

Now again let $v_i, v_j, v_{i,j}$ be vectors spanning p'_i, p'_j and $l'_i \cap l'_j$ respectively. Then let $s_{i,j}(t)$ and $b_{i,j}(t)$ be the transformations from above for \mathcal{F}_4^+ , represented in the basis $(v_i, v_{i,j}, v_j)$. Analogue to the previous case set

$$\begin{aligned} N_{i,j}(t) &:= (s_{i,j}(t) \cdot N_L) \cup (s_{i,j}(-t) \cdot N_R) \\ N'_{i,j}(t) &:= (s_{i,j}(t) \cdot N'_L) \cup (s_{i,j}(-t) \cdot N'_R) \\ M_{i,j}(t) &:= (b_{i,j}(t) \cdot N_L) \cup (b_{i,j}(-t) \cdot N_R) \\ M'_{i,j}(t) &:= (b_{i,j}(t) \cdot N'_L) \cup (b_{i,j}(-t) \cdot N'_R) \end{aligned}$$

With this we can define the analogue flows on \mathcal{F}_n^+ .

Definition 4.1.3. Let $a_{i,j}$ be an internal edge. Then

1) The **shearing flow** on \mathcal{F}_n^+ associated to $a_{i,j}$ is the flow

$$(\gamma_{i,j})_t : \mathcal{F}_n^+ \longrightarrow \mathcal{F}_n^+, (N, N') \mapsto (N_{i,j}(t), N'_{i,j}(t))$$

2) The **bulging flow** on \mathcal{F}_4^+ associated to $a_{i,j}$ is the flow

$$(\beta_{i,j})_t : \mathcal{F}_n^+ \longrightarrow \mathcal{F}_n^+, (N, N') \mapsto (M_{i,j}(t), M'_{i,j}(t))$$

With the same argument as before we get the following:

Lemma 4.5. *The shearing and bulging flows on \mathcal{F}_n^+ are well defined.*

After defining the flows above which transform the coordinates defined using the cross ratio we also want to see if we can do a similar thing for the triple ratio of the triangles in the triangulation of N .

Therefore consider $i, j, k = 1, \dots, n$ so that $i < j < k$ and let

$$p_1 := p'_i, p_2 := p'_j, p_3 := p'_k$$

Now the three edges $a_{i,j}, a_{j,k}$ and $a_{k,i}$ cut N' into four polygons M'_1, M'_2, M'_3 and Δ where M'_i has $a_{i-1, i+1}$ as an edge and Δ has vertices p_1, p_2, p_3 .

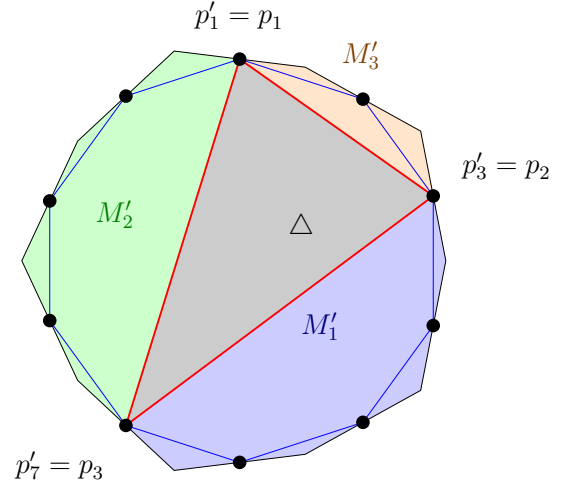


Figure 4.8: Decomposition into four polygons for $i, j, k = 1, 3, 7$.

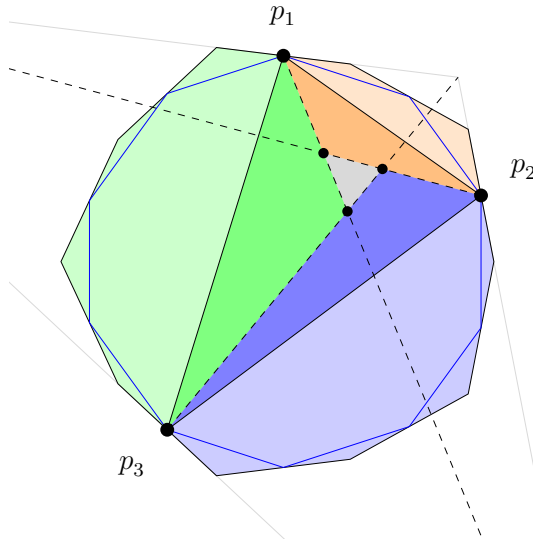


Figure 4.9: N'_1 in blue with M'_1 less opaque. Same for N'_2 (green) and N'_3 (orange)

Set u_1, u_2, u_3 as in notation 2.3.3 and let T_i be the triangle in Δ with vertices p_{i-1}, u_i, p_{i+1} .

Now if we denote $N'_i := M'_i \cup T_i$ then $N' = T \cup N'_1 \cup N'_2 \cup N'_3$ if T is the triangle in Δ with vertices u_1, u_2, u_3 . Similarly, the three edges cut N into four polygons. Let M_i be such that $N = \Delta \cup M_1 \cup M_2 \cup M_3$ enumerated like the M'_i . Then also $N = T \cup N_1 \cup N_2 \cup N_3$.

Now if $p_1 := p'_i, p_2 := p'_j, p_3 := p'_k$ we define $(q_i)_{i=1,2,3}$ like in subsection 4.1.1, choose the basis (q_1, q_2, q_3) and define the maps $g_1(t), g_2(t), g_3(t) \in \text{PGL}(3, \mathbb{R})$. Then define

$$\begin{aligned} N_{i,j,k}(t) &:= (g_1(t) \cdot N_1) \cup (g_2(t) \cdot N_2) \cup (g_3(t) \cdot N_3) \cup T(t) \\ N'_{i,j,k}(t) &:= (g_1(t) \cdot N'_1) \cup (g_2(t) \cdot N'_2) \cup (g_3(t) \cdot N'_3) \cup T(t) \end{aligned}$$

Like before the pair $(N_{i,j,k}(t), N'_{i,j,k}(t))$ is a pair of suitably nested polygons.

Definition 4.1.4. The **eruption flow** on \mathcal{F}_n^+ associated to p_i, p_j, p_k is the flow

$$(\varepsilon_{i,j,k})_t : \mathcal{F}_n^+ \longrightarrow \mathcal{F}_n^+, \quad (N, N') \mapsto (N_{i,j,k}(t), N'_{i,j,k}(t))$$

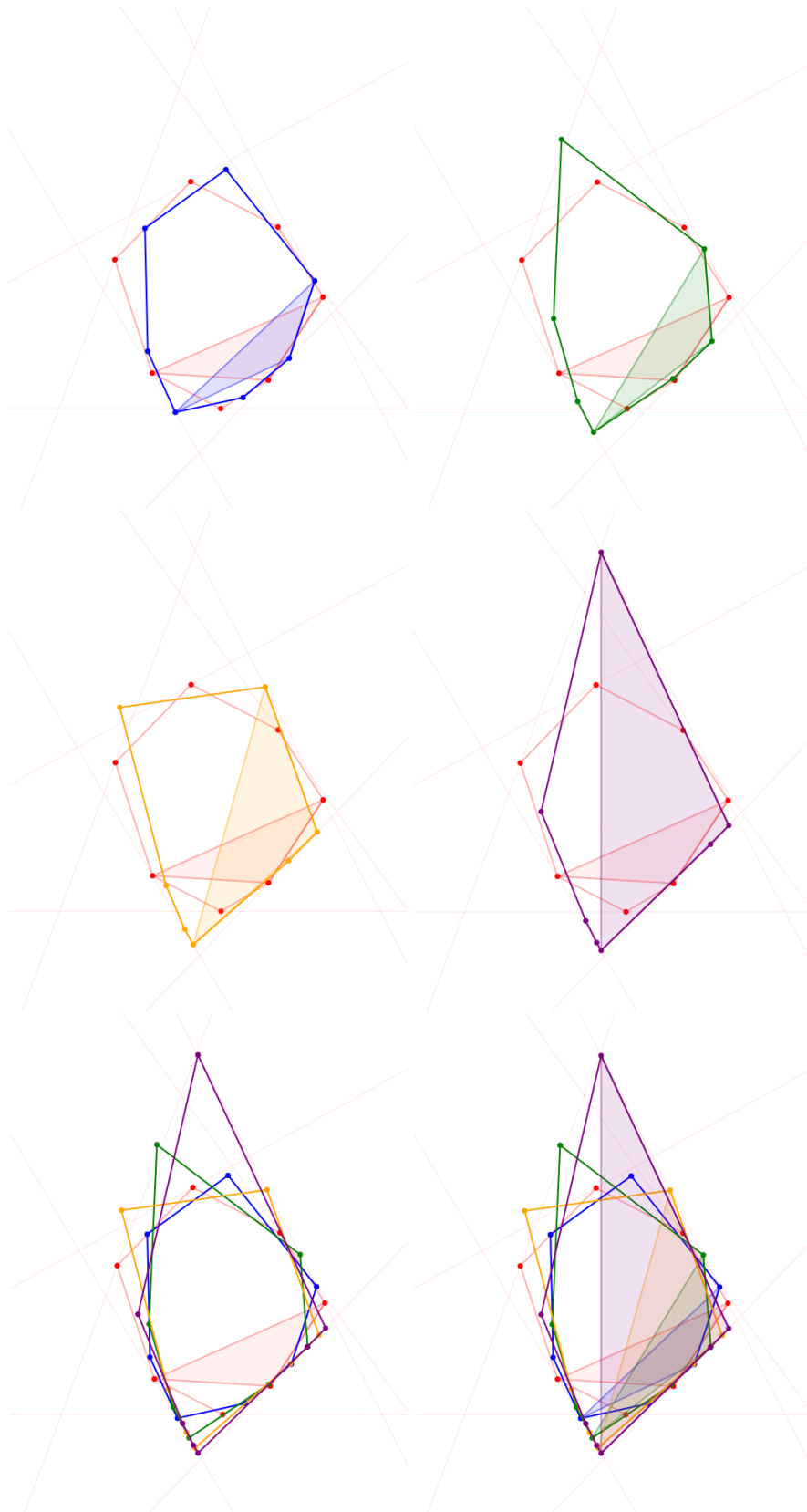


Figure 4.10: Eruptions on a 7-gon in \mathcal{F}_7^+ associated to the drawn triangle for $t = 2, 4, 6, 8$. The last two images show all values at once.

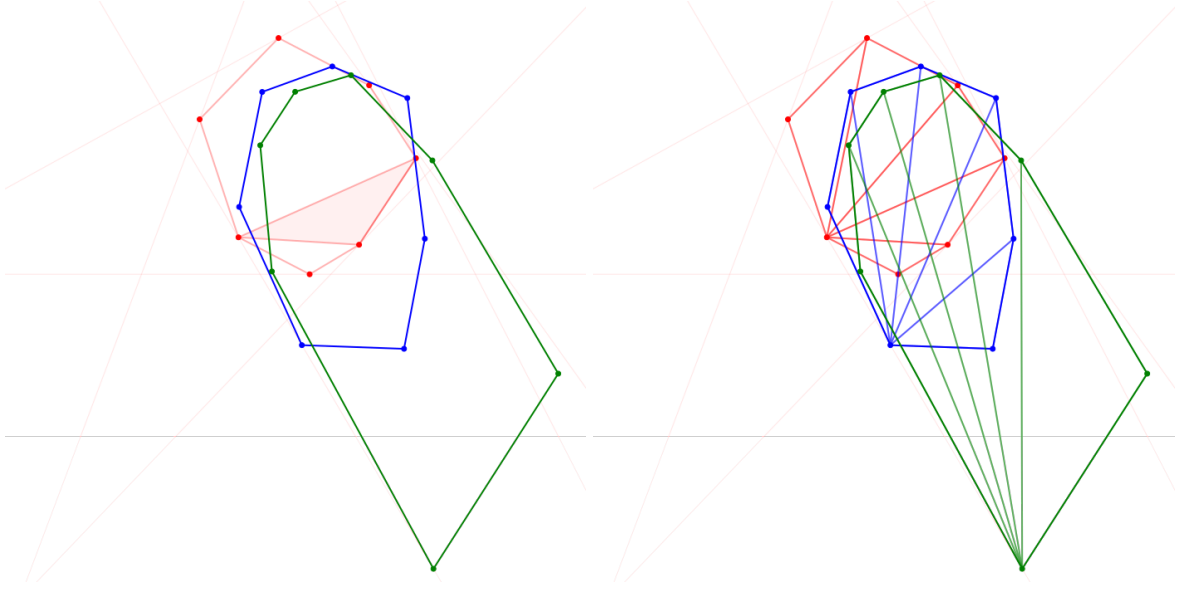


Figure 4.11: Erruptions on a 7-gon in \mathcal{F}_7^+ associated to all triangles for $t = 0.2, 0.4$.

Thus we have generalized all flows to \mathcal{F}_n^+ . Let $(N, N') = ((\bar{p}_1, \bar{l}_1), \dots, (\bar{p}_n, \bar{l}_n)) \in \mathcal{F}_n^+$ and let \mathcal{T} be a triangulation of N such that the set of vertices of the triangulation is $\{\bar{p}_1, \dots, \bar{p}_n\}$. Again let $I_{\mathcal{T}}$ be the set of internal edges of \mathcal{T} and let $\Theta_{\mathcal{T}}$ be the set of triangles of \mathcal{T} . The erruption, shearing and bulging flows, associated to a triangulation of N , descend naturally to flows on $\text{PGL}(3, \mathbb{R}) \setminus \mathcal{F}_n^+$. Those flows have the following properties.

Proposition 4.6. *Consider the collection of flows on $\text{PGL}(3, \mathbb{R}) \setminus \mathcal{F}_n^+$*

$$\mathcal{M}(\mathcal{F}_n^+) := \{\gamma_{i,j} | a_{i,j} \in I_{\mathcal{T}}\} \cup \{\beta_{i,j} | a_{i,j} \in I_{\mathcal{T}}\} \cup \{\varepsilon_{i,j,k} | \{a_{i,j}, a_{j,k}, a_{k,i}\} \in \Theta_{\mathcal{T}}\}$$

Then

- 1) For any $\phi_1, \phi_2 \in \mathcal{M}(\mathcal{F}_n^+)$ and any $t_1, t_2 \in \mathbb{R}$ $(\phi_1)_{t_1}(\phi_2)_{t_2} = (\phi_2)_{t_2}(\phi_1)_{t_1}$ as flows on $\text{PGL}(3, \mathbb{R}) \setminus \mathcal{F}_n^+$
- 2) For any pair $F_1, F_2 \in \text{PGL}(3, \mathbb{R}) \setminus \mathcal{F}_n^+$ there is a sequence $\phi_1, \dots, \phi_m \in \mathcal{M}(\mathcal{F}_n^+)$ and a sequence $t_1, \dots, t_n \in \mathbb{R}$ such that $F_1 = (\phi_1)_{t_1} \circ \dots \circ (\phi_n)_{t_n}(F_2)$.

Proof. These proofs follow directly from the parametrization of \mathcal{F}_n^+ and the fact that the above flows change specific coordinates each. \square

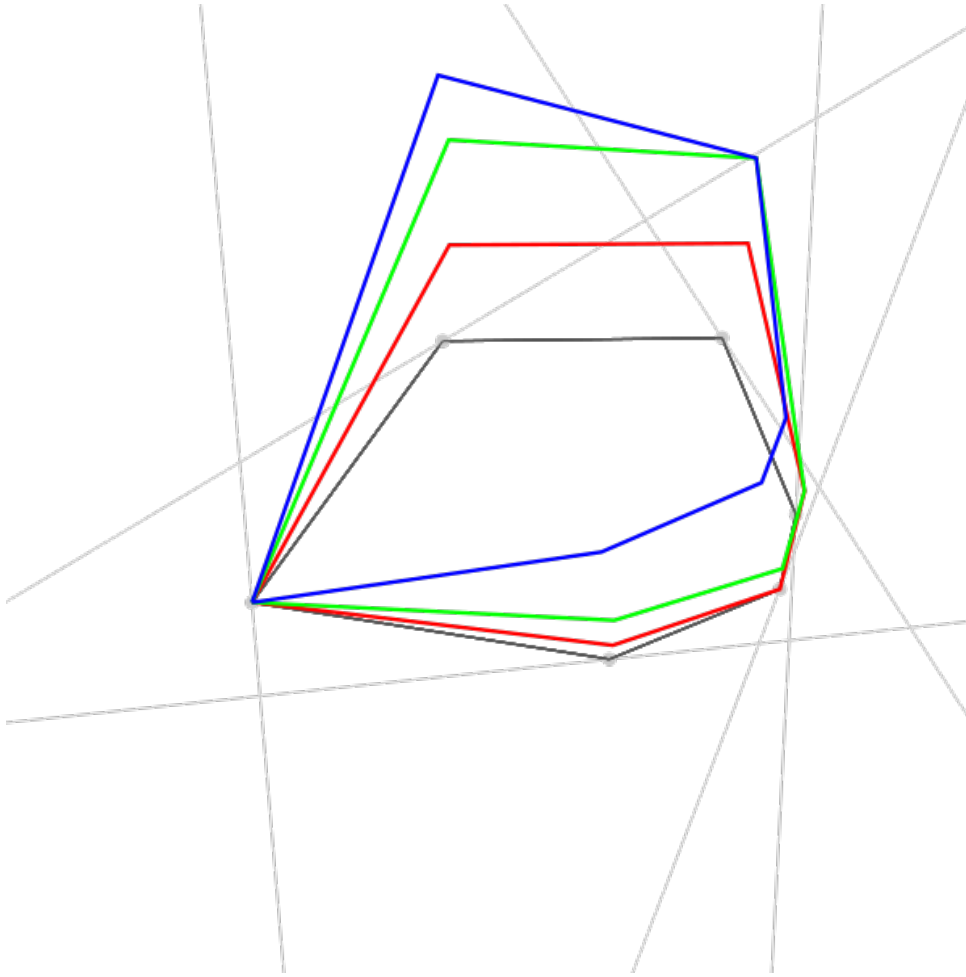


Figure 4.12: Bulging of a 6-gon at all internal edges with $t = 0.5$. The colours show the deformation after using 1,2 or all 3 internal edges (red to blue).

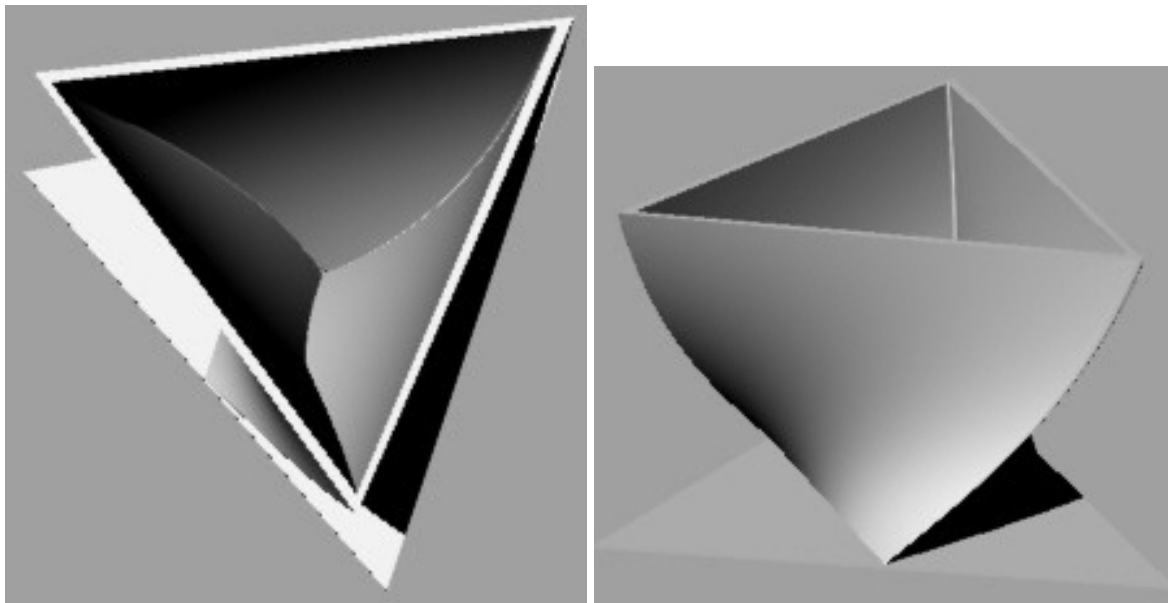


Figure 4.13: Eruption flow on \mathcal{F}_3^+ visualized in 3D.

4.2 Deformations of convex sets

In this section we want to discuss how to define the introduced flows on properly convex sets. We will give two approaches. The first will be a generalization of the results for elements in \mathcal{F}_n^+ . The second approach will apply the flows for flags on sets created by tilings via polygons.

4.2.1 With C^1 -boundary (general)

This subsection will give the rough outline on how to generalize the ideas from the deformations or flows on \mathcal{F}_n^+ to proper convex sets with C^1 -boundary. This will help understand the following set:

$$\mathcal{D} := \{(\xi, \Omega) \mid \Omega \subset \mathbb{RP}^2 \text{ strictly convex with } C^1 \text{ boundary, } \xi : S^1 \longrightarrow \partial\Omega \text{ homeom.}\}$$

To be able to state the results we introduce some notation. This will follow chapter 4 of [WZ18].

- Notation 4.2.1.**
- For pairwise distinct $x, y, z \in S^1$ in that order let $[x, y]_z$ and $(x, y)_z$ be the closed and open subintervals of S^1 with endpoints x, y that do not contain z .
 - For any properly convex domains $\Omega \subset \mathbb{RP}^2$ and $a, b \in \bar{\Omega}$ let $[a, b]$ and (a, b) be the closed and open oriented projective line segments in Ω with a, b as backward and forward points.
 - For $p, q \in \mathbb{RP}^2$ let \overline{pq} be the projective line through p and q
 - For any $(\xi, \Omega) \in \mathcal{D}$ and for $x \in S^1$ let $\xi^*(x)$ be the tangent line to $\partial\Omega$ at $\xi(x)$

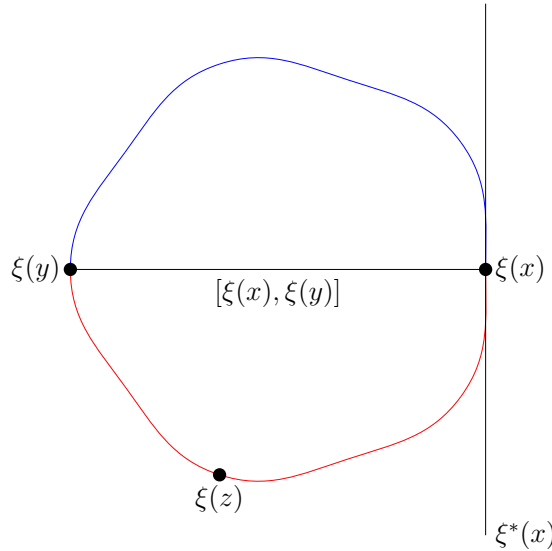


Figure 4.14: Notation on a convex set with C^1 -boundary. $[\xi(x), \xi(y)]_{\xi(z)}$ in blue.

We will start by defining the bulging and shearing flow in this case. Let $x, y \in S^1$ be a pair of distinct points. Then $[\xi(x), \xi(y)]$ cuts Ω in two properly convex domains $\Omega_{x,y,L}$ and $\Omega_{x,y,R}$ which lie left and right of $[\xi(x), \xi(y)]$. The orientation is induced by ξ . Let $p_{x,y}$ be the

intersection of $\xi^*(x)$ and $\xi^*(y)$. If we now choose the basis $(\xi(x), p_{x,y}, \xi(y))$ we define the maps

$$s_{x,y}(t) = \begin{bmatrix} e^{t/2} & 0 & 0 \\ 0 & 1 & 0 \\ 0 & 0 & e^{-t/2} \end{bmatrix} \quad b_{x,y}(t) = \begin{bmatrix} e^{-t/6} & 0 & 0 \\ 0 & e^{t/3} & 0 \\ 0 & 0 & e^{-t/6} \end{bmatrix}$$

It is easy to check that each $g \in \text{PGL}(3, \mathbb{R})$ that fixes the basis above can be written as a product $s_{x,y}(t_1)b_{x,y}(t_2)$. This follows directly from the fact that elements acting on the basis act on the maps above by conjugation.

Now let $g_{t_1,t_2} := s_{x,y}(t_1)b_{x,y}(t_2)$ for $t_1, t_2 \in \mathbb{R}$. Then for any $g = g_{t_1,t_2}$ let

$$\Omega_g := (\xi(x), \xi(y)) \cup (g \cdot \Omega_{x,y,L}) \cup (g^{-1}\Omega_{x,y,R})$$

and if B_L and B_R are the components of $S^1 \setminus \{x, y\}$ such that $\xi(B_L)$ and $\xi(B_R)$ are the boundaries of $\Omega_{x,y,L}$ and $\Omega_{x,y,R}$ let

$$\xi_g(a) = \begin{cases} g \circ \xi(a) & a \in B_L \\ g^{-1} \circ \xi(a) & a \in B_R \\ \xi(a) & a = x, y \end{cases}$$

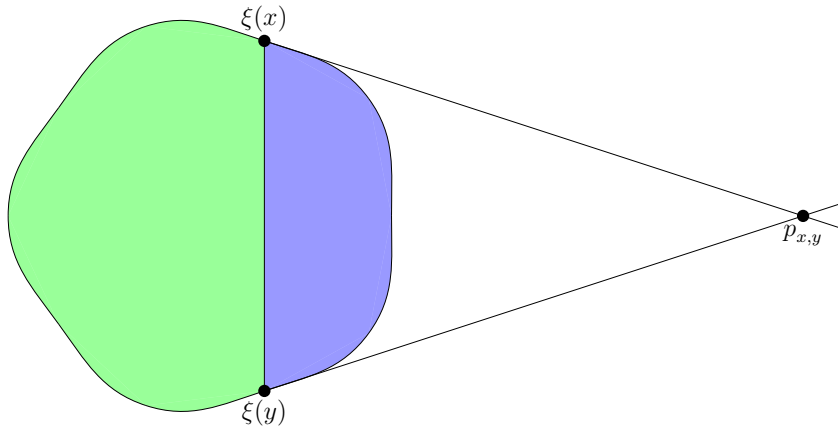


Figure 4.15: Data for shearing and bulging flow on convex sets with C^1 boundary. $\Omega_{x,y,L}$ in blue and $\Omega_{x,y,R}$ in green.

Note that Ω_g is also strictly convex with C^1 -boundary and that ξ_g is continuous. Thus we can define:

Definition 4.2.2. Let $x, y \in S^1$. Then

1) the **elementary shearing flow** on \mathcal{D} associated to (x, y) is the flow

$$(\gamma_{x,y})_t : \mathcal{D} \longrightarrow \mathcal{D}, (\xi, \Omega) \mapsto (\xi_{s_{x,y}(t)}, \Omega_{s_{x,y}(t)})$$

2) the **elementary bulging flow** on \mathcal{D} associated to (x, y) is the flow

$$(\beta_{x,y})_t : \mathcal{D} \longrightarrow \mathcal{D}, (\xi, \Omega) \mapsto (\xi_{b_{x,y}(t)}, \Omega_{b_{x,y}(t)})$$

We note that these flows commute with elements in $\text{PGL}(3, \mathbb{R})$ and thus descend to flows on $\text{PGL}(3, \mathbb{R}) \setminus \mathcal{D}$. Analogue to the known behaviour for flags we want to use cross ratios to get some characteristic values for Ω . For this we consider $(\xi, \Omega) \in \mathcal{D}$ and for any $y_1 < z_1 < y_2 < z_2 < y_1$ along S^1 in the cycling order we define

$$\sigma_\xi(y_1, z_1, z_2, y_2) := \log \left(-C \left(\xi^*(y_1), \xi(z_1), \xi(z_2), \overline{\xi(y_1)\xi(y_2)} \right) \right).$$

This is well defined and allows us to investigate the change made by the bulging and shearing flows.

Proposition 4.7. *Let $y_1 \neq y_2 \in S^1$ and for $i = L, R$ let $z_i \in B_i$ with respect to the oriented line segment $[y_1, y_2]$. Furthermore let $(\xi_1, \Omega_1) := (\gamma_{y_1, y_2})_t(\xi, \Omega)$ and $(\xi_2, \Omega_2) := (\beta_{y_1, y_2})_t(\xi, \Omega)$. Then*

- 1) $\sigma_{\xi_1}(y_1, z_L, z_R, y_2) = \sigma_\xi(y_1, z_L, z_R, y_2) - t$,
- 2) $\sigma_{\xi_1}(y_2, z_R, z_L, y_1) = \sigma_\xi(y_2, z_R, z_L, y_1) - t$,
- 3) $\sigma_{\xi_1}(y_1, z_L, z_R, y_2) = \sigma_\xi(y_1, z_L, z_R, y_2) + t$,
- 4) $\sigma_{\xi_1}(y_2, z_R, z_L, y_1) = \sigma_\xi(y_2, z_R, z_L, y_1) - t$.

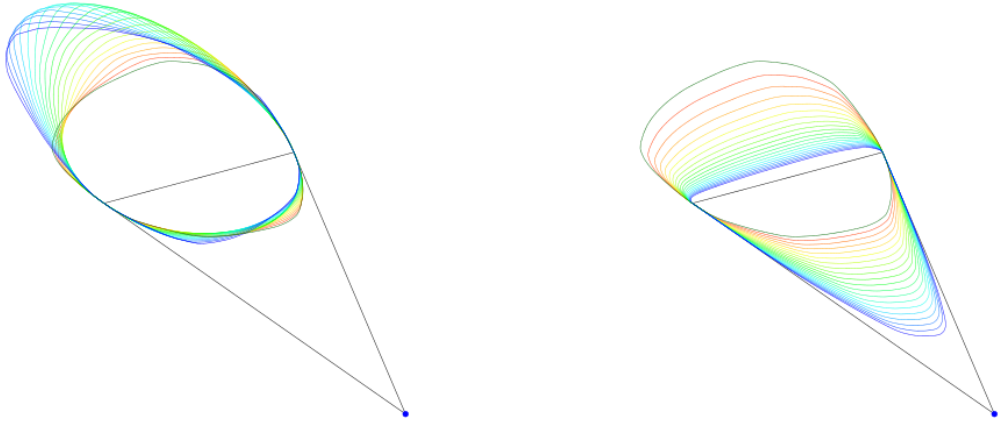


Figure 4.16: Shearing (left) and bulging associated to the drawn line.

To complete the triple of flows we now consider the eruption flow. Therefore let $x, y, z \in S^1$ be pairwise distinct and $(\xi, \Omega) \in \mathcal{D}$. Let $p_1 = \xi(x), p_2 = \xi(y), p_3 = \xi(z)$ and $l_1 = \xi^*(x), l_2 = \xi^*(y), l_3 = \xi^*(z)$. This defines us three flags from which we can construct a triangle T with vertices u_1, u_2, u_3 (see Notation 2.3.3). Denote by Ω_i the subdomain of Ω bounded by $[p_{i-1}, p_{i+1}]_{p_i}, [p_{i-1}, u_i]$ and $[u_i, p_{i+1}]$. Then

$$\Omega = \Omega_1 \cup \Omega_2 \cup \Omega_3 \cup T$$

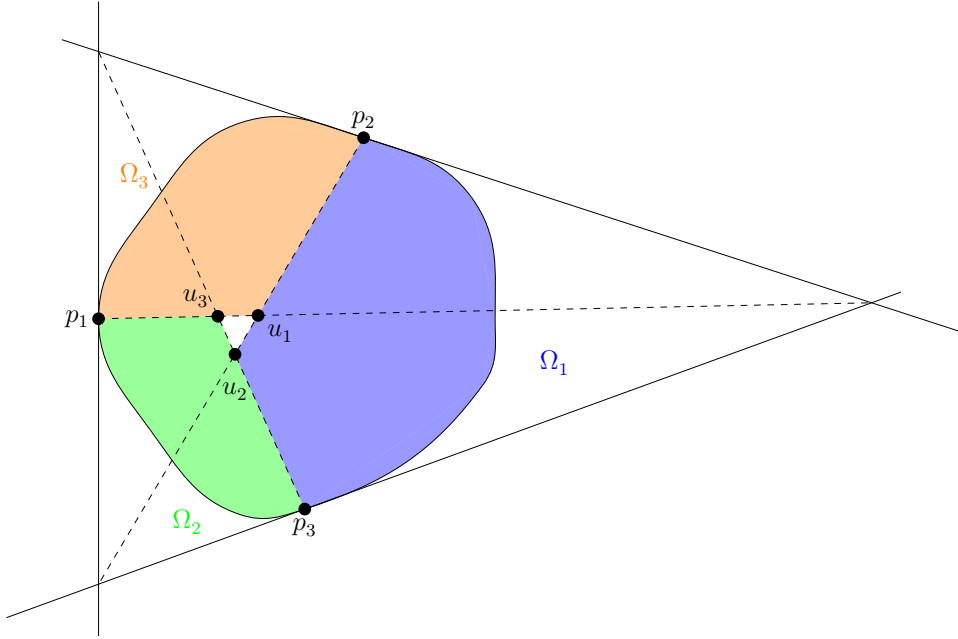


Figure 4.17: Data for eruption flow on convex sets with C^1 boundary.

Again we can define the maps $g_1, g_2, g_3 \in \text{PGL}(3, \mathbb{R})$ (see subsection 4.1.1) and by the same argument as before there is a unique triangle $T(t)$ such that

$$\Omega_{x,y,z,t} := (g_1(t) \cdot \Omega_1) \cup (g_2(t) \cdot \Omega_2) \cup (g_3(t) \cdot \Omega_3) \cup T(t)$$

which is strictly convex with C^1 boundary. Also the tangent to $\Omega_{x,y,z,t}$ at i.e. $g_1(s)\xi(x)$ is l_1 . Similarly for y, z . We can also define a continuous $\xi_{x,y,z,t} : S^1 \rightarrow \partial\Omega_{x,y,z,t}$ by

$$\xi_{x,y,z,t}(a) = \begin{cases} g_1(t)\xi(a) & a \in [y, z]_x \\ g_2(t)\xi(a) & a \in [z, x]_y \\ g_3(t)\xi(a) & a \in [x, y]_z \end{cases}$$

This results in

Definition 4.2.3. Let $x, y, z \in S^1$ be a triple of pairwise distinct points. The **elementary eruption flow** on \mathcal{D} associated to x, y, z is the flow

$$(\varepsilon_{x,y,z})_t : \mathcal{D} \rightarrow \mathcal{D}; (\xi, \Omega) \mapsto (\xi_{x,y,z,t}, \Omega_{x,y,z,t})$$

Because this flow also commutes with elements in $\text{PGL}(3, \mathbb{R})$ it descends to the flow on $\text{PGL}(3, \mathbb{R}) \setminus \mathcal{D}$.

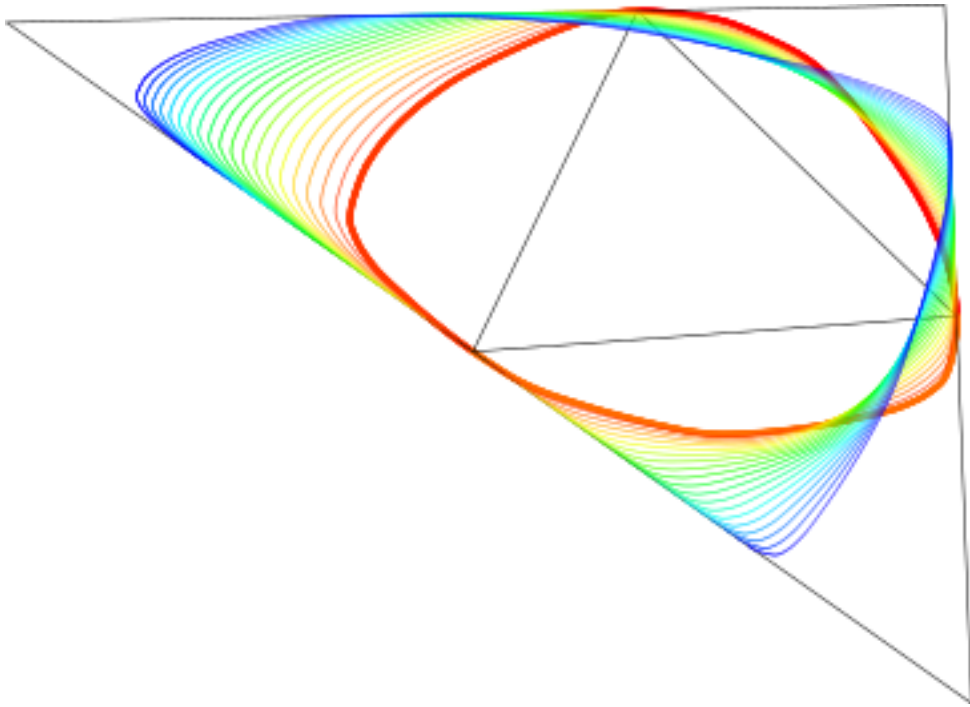


Figure 4.18: Eruption flow on convex sets with C^1 boundary for $t = 0$ to $t = 4$ (red to blue).

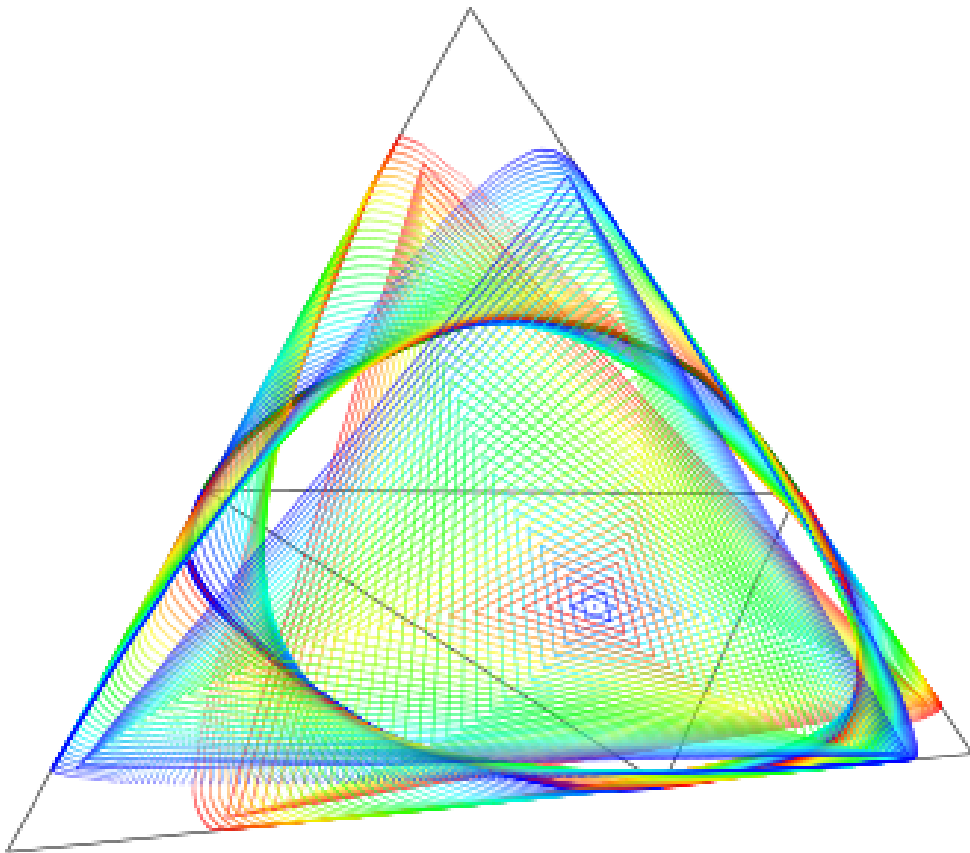


Figure 4.19: Eruption flow on convex sets with C^1 boundary for $t = -6$ to $t = 6$. We include this image just because it looks nice.

To finish this subsection we will also define an appropriate function here and state how the eruption flow changes this parameter. Consider

$$\tau_\xi(x, y, z) := \log T((\xi^*(x), \xi(x)), (\xi^*(y), \xi(y)), (\xi^*(z), \xi(z))).$$

This is well defined since this triple ratio is always positiv (see [WZ18]). Then

Proposition 4.8. *Let $x, y, z \in S^1$ and let $(\xi, \Omega) \in \mathcal{D}$. For all $t \in \mathbb{R}$ let $(\varepsilon_{x,y,z})_t(\xi, \Omega) = (\xi_1, \Omega_1)$. Then*

$$\tau_{\xi_1}(x, y, z) = \tau_\xi(x, y, z) + t$$

4.2.2 Constructed from tilings

Here we try to apply the defined flows on the convex sets Ω which we build from the reflection group of the suitably nested polygon P of an element $F \in \mathcal{F}_n^+$. The goal is to define the transformations in a way such that the group action is preserved. Consider a 4-gon in \mathcal{F}_4^+ and a reflection σ along one edge (associated to Ω). Then by applying the bulging flow on the initial 4-gon we get a configuration where the original and the reflected 4-gon are not equivalent up to $\text{PGL}(3, \mathbb{R})$ since the internal parameters of the two polygons are different.



Figure 4.20: Applying the a bulge transformation associated to the red line will change the inner parameters of the gray 4-gon but not of the blue 4-gon.

To tackle this problem we have two strategies:

- 1) apply the flow associated to an internal edge and all its reflections,
- 2) apply the flow and then reflect using new reflections constructed from the new configuration.

The second approach is a lot easier with regard to the visualization process and creates a set Ω' such that the reflection group of the transformed polygon acts nicely on it. The first approach is harder to program but is the general method used to get the desired property, i.e. that Ω is Γ -invariant if Γ is the group generated from the reflections.

To understand if these two processes are related we will investigate it for $F \in \mathcal{F}_4^+$ with suitably nested polygons (N, N') . For a 4-gon the reflection group is represented by

$$\Gamma = \langle R_1, R_2, R_3, R_4 | \cdot \rangle$$

and we omit the relations since they won't change and thus are not important for our observations.

First of we consider approach 2), i.e. we first transform our polygon and then apply the reflection group generated from the reflections of the transformed polygon. Let us first consider bulging and shearing flows, so choose a triangulation and without loss of generality let $a_{1,3}$ be the internal edge. Let g be one of the two transformations associated to $a_{1,3}$ and R_i be the reflections along the edges in figure 4.21.

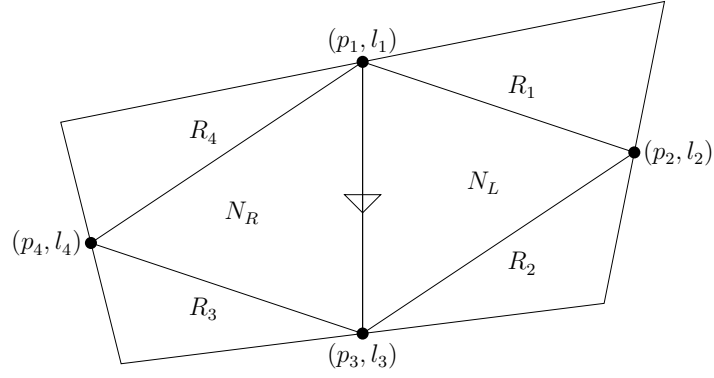


Figure 4.21: Decomposition of $F \in \mathcal{F}_4^+$ with triangulation and internal edge.

In approach 2) we only apply g once and thus the new reflection group is given by the following generators:

$$\begin{aligned} R_1 &\mapsto g(t)R_1g(t)^{-1} =: R_1^g \\ R_2 &\mapsto g(t)R_2g(t)^{-1} =: R_2^g \\ R_3 &\mapsto g(t)^{-1}R_3g(t) =: R_3^g \\ R_4 &\mapsto g(t)^{-1}R_4g(t) =: R_4^g \end{aligned}$$

We can see this as follows: the reflection R_i is generated using the points p_i, p_{i+1} and $l_i \cap l_{i+1}$. Since linear forms change under the rule $\alpha \mapsto \alpha g^{-1}$ if points change by $v \mapsto gv$ we get the new reflection, e.g. R_1' , via:

$$R_1' = \text{Id} - \alpha_1 g^{-1}(t) \otimes g(t)v_1 = \text{Id} - g(t)v_1 \alpha_1 g^{-1}(t) = g(t) [\text{Id} - v_1 \alpha_1] g^{-1}(t) = g(t)R_1g^{-1}(t)$$

Note here that because all the needed data always lies on one side of $a_{1,3}$ this conjugation works. For the eruption flow it is the same argument in this case, except g is a product of eruption transformations on both of the triangles.

Now let us consider approach 1), i.e. we apply the flows on each $\gamma(F)$ for $\gamma \in \Gamma$. For now we consider only bulging and shearing deformations.

Since it is trickier to work with transformations that act differently depending on which side of $a_{1,3}$ we consider we use the following trick: we are only interested in the configuration of the flags and we know that this is invariant under $\text{PGL}(3, \mathbb{R})$. So after applying the bulging or shearing transformations we can, globally, apply an element in $h \in \text{PGL}(3, \mathbb{R})$ and the configuration does not change. By choosing h to be one of the transformations $g(t)$ or $g(-t)$ we achieve that the bulging flow is the identity on one side of $a_{1,3}$ and $g(\pm 2t)$ on the other side.

We start by investigating the situation for the reflection R_1 defined by the line through p_1 and p_2 and the fix point $q_1 = l_1 \cap l_2$. To get a good graphical understanding we choose an affine chart such that $q_1 = \infty$ which results in l_1 and l_2 being parallel and R_1 being a euclidean reflection.

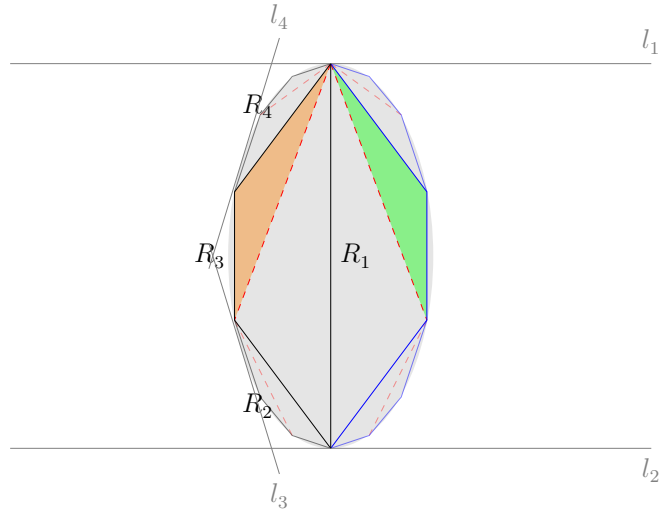


Figure 4.22: Deforming the nested 4-gons in a suitable chart. N in black, $R_1(N)$ in blue

So, applying g associated to $a_{1,3}$ on N such that only the outer half changes (shaded orange in figure 4.22), denoted by g_0 , and then doing the same on $R_1(N)$ (shaded in green), denoted by g_1 , we obtain two new 4-gons having the same configuration and still being related by R_1 . Through this process we get new reflections

$$\begin{aligned} R_1 &\mapsto \text{Id}R_1\text{Id} \mapsto \text{IdId}R_1\text{IdId} = R_1 \\ R_2 &\mapsto \text{Id}R_2\text{Id} \mapsto \text{IdId}R_2\text{IdId} = R_2 \\ R_3 &\mapsto g_0(-2t)R_3g_0(2t) \mapsto \text{Id}g_0(-2t)R_3g_0(2t)\text{Id} = g_0(-2t)R_3g_0(2t) \\ R_4 &\mapsto g_0(-2t)R_4g_0(2t) \mapsto \text{Id}g_0(-2t)R_4g_0(2t)\text{Id} = g_0(-2t)R_4g_0(2t) \end{aligned}$$

It is important to note here that g_1 does not change anything.

Bulging or shearing along an edge $\gamma(a_{1,3})$ will not change the configuration of N and using suitable affine charts we see that all four new generators are indeed reflections. Note that we always bulge or shear outward, i.e. we choose the transformation in such a way that N is transformed by the identity map. Thus we obtain the following:

Claim 4.9. *Consider bulging or shearing transformations. Let Γ_1, Γ_2 be the reflection groups attained through approach 1) or 2) respectively and Ω_1, Ω_2 the convex sets obtained as union of the respective orbits. Then they are equal.*

One observation to make here is that the vertices of each $\gamma(N)$ are part of $\partial\Omega$. This is immediately clear from the construction of these sets if you consider the images of the flags and the fact that the group action tiles a half space. Thus, taking the convexity into account, every inner edge splits Ω into exactly two components and each triangle cuts it into 3 components plus the triangle. This makes sure that N is fixed by all transformations on the $\gamma(N)$, $\gamma \neq \text{Id}$.

For the eruption flow the same process should work. Observe that the transformation can be chosen to be the identity on one of the three polygons of $N' \setminus \Delta$ where Δ is the triangle associated to the eruption transformation. Thus we claim the following:

Claim 4.10. *Let $F \in \mathcal{F}_n^+$ and g be one of the discussed transformations. Let Γ_1, Γ_2 be the reflection groups attained through approach 1) or 2) respectively and Ω_1, Ω_2 the convex sets obtained as union of the respective orbits. Then $\Gamma_1 = \Gamma_2$ and $\Omega_1 = \Omega_2$.*

To end this discussion we want to consider the trick used above shortly. As explained before the idea is to transform the whole set Ω by $g(t)$ or $g(-t)$ directly after applying the transformation on each of the components. For example let N_L, N_R be the left and right side according to an internal edge. Then we do the following steps:

$$(N_L, N_R) \mapsto (g(t)N_L, g(-t)N_R) \mapsto (g(t)g(t)N_L, g(t)g(-t)N_R) = (g(2t)N_L, N_R)$$

Effectively we choose, in each $\gamma(N)$, a suitable representative for current class in $\mathrm{PGL}(3, \mathbb{R}) \setminus \mathcal{F}_n^+$. In the end we obtain a Γ -invariant convex set Ω whose fundamental domain N has the desired parameters.

Approach 2) yields the following pictures for example:

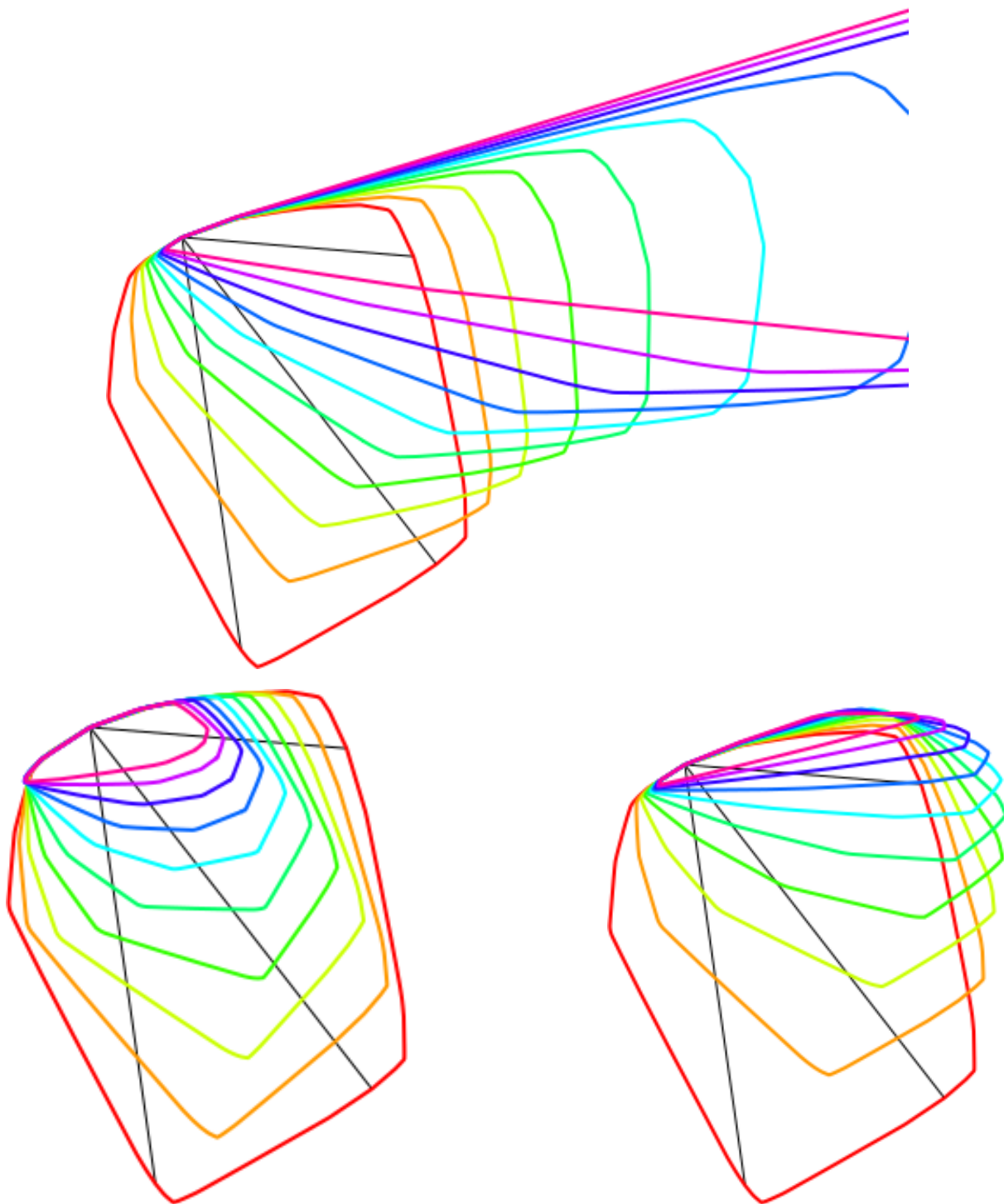


Figure 4.23: Transforming the red convex set by applying transformations associated to the black edges. Top: bulge, left: shear, right: bulge and shear. Each 10 times for $t = 0$ to $t = 0.9$ (red to green to purple).

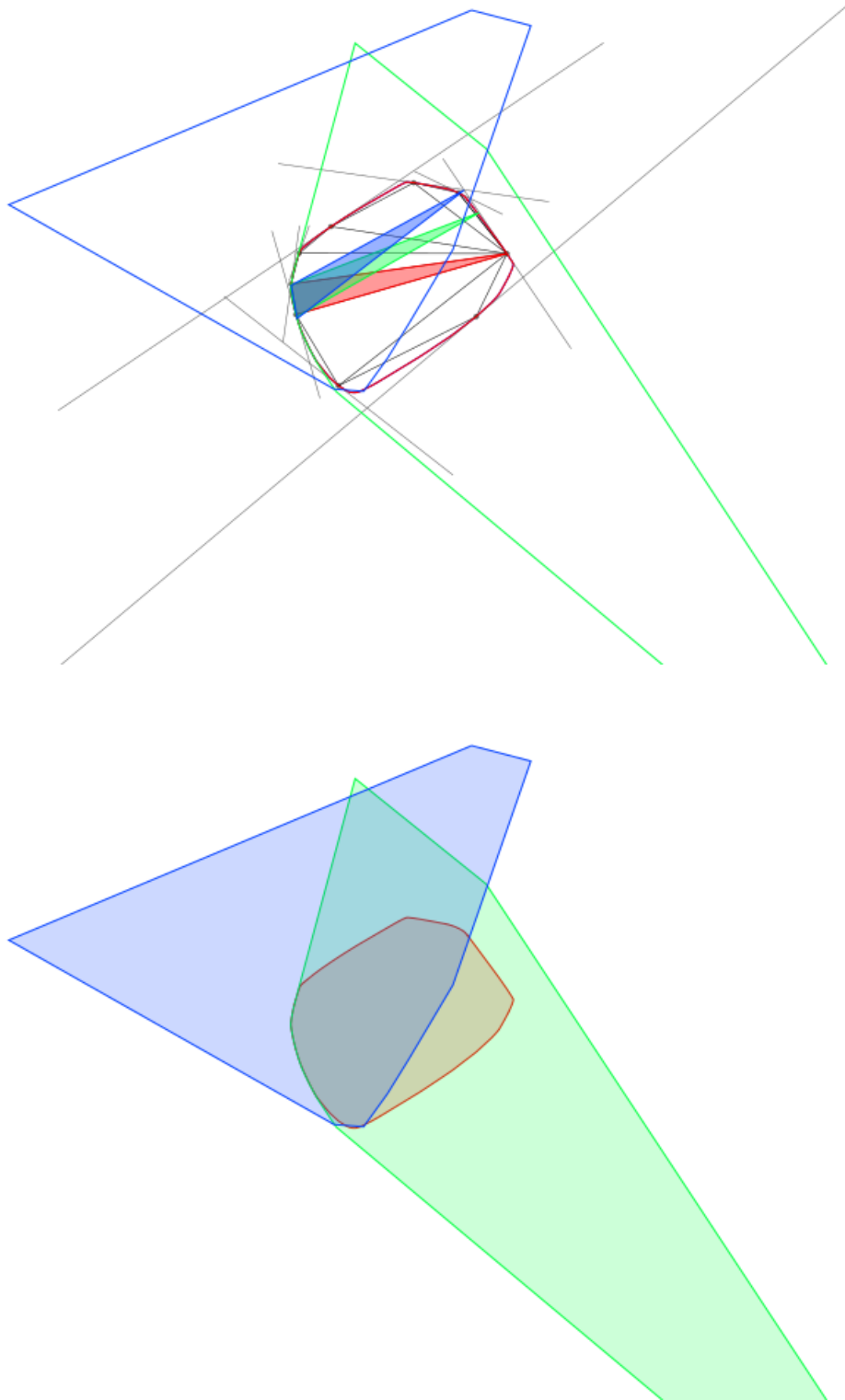


Figure 4.24: Eruption flow on a 9-gon associated to one triangle. Drawn for $t = 0, 0.3, 0.5$ (red, green, blue).

5 Visualization

In this chapter we take a look at visualizing the theory of the previous chapters. We will give tips and computations on how to draw explicit pictures.

5.1 \mathbb{RP}^2 and affine charts

First of all we take a short look at ways to visualize objects in projective plane. If we see \mathbb{RP}^2 as the space of 1-dimensional subspaces of \mathbb{R}^3 we can choose representatives in many ways. But since we want to generate images it is important to find some good representatives that lie on a plane.

The most common way there is to use **homogenous coordinates**. Here we think of the projective plane as the euclidean plane together with a set of directions. Every point $(x, y) \in \mathbb{R}^2$ can be seen as a point $(x, y, 1) \in \mathbb{R}^3$. These points are representatives for lines in \mathbb{R}^3 which do not lie in the xy -plane $z = 0$. Like this we can draw most of the projective plane which is often enough. The essence here is that we need to ignore a 2-dimensional subspace in \mathbb{R}^3 to visualize the rest. Furthermore, to generate images from 3D data it is often the easiest to just ignore one of the 3 coordinates.

So given the unit normal $n = (n_1, n_2, n_3)$ of the 2-dimensional subspace E we want to do this:

1. Make sure $n_3 \geq 0$ (to simplify the rotation later on)
2. For every point $L \in \mathbb{RP}^2$ such that the corresponding line is not in E find the representative $x \in \mathbb{R}^3$ in $n + E$
3. Compute the 3D-rotation R_{e_3} that sends n to e_3
4. Map the plane $n + E$ to the xy -plane via: $x \mapsto R_{e_3}(x - n)$

Then we can simply generate the image using the first two coordinates of the points. We now cover some details for this algorithm:

1. If $n_3 < 0$ simply multiply everything with $-\text{Id}$
2. Every 2d subspace E can be written as the set of points solving

$$\langle n, x \rangle = \left\langle \begin{pmatrix} n_x \\ n_y \\ n_z \end{pmatrix}, \begin{pmatrix} x \\ y \\ z \end{pmatrix} \right\rangle = n_x x + n_y y + n_z z = 0$$

where n is the unit normal of the plane. The idea now is to glue a parallel copy of E on the sphere at n . A point $A = (a \ b \ c)$ lies on the plane $n + E$ if and only if

$$\begin{pmatrix} a \\ b \\ c \end{pmatrix} - n \in E \Leftrightarrow \langle n, A - n \rangle = 0 \Leftrightarrow \langle n, A \rangle - \langle n, n \rangle = 0 \Leftrightarrow \langle n, A \rangle = 1$$

So, given a line L in $\mathbb{R}^3 \setminus E$ choose a representative $x \in \mathbb{R}^3$ such that $[x] = L$ in \mathbb{RP}^2 . Now the representative in $n + E$ is given by $\frac{x}{\langle n, x \rangle}$.

3. We will compute the general case here: find the rotation in \mathbb{R}^3 that sends a unit vector P to a unit vector Q .

This is simply a rotation around the normal of the plane spanned by P and Q . We will make use of the cross product for this.

First consider a rotation in the xy -plane:

$$G = \begin{pmatrix} \cos(\alpha) & -\sin(\alpha) & 0 \\ \sin(\alpha) & \cos(\alpha) & 0 \\ 0 & 0 & 1 \end{pmatrix}$$

Using the cross product to deduce the angle of rotation this becomes

$$G = \begin{pmatrix} \langle P, Q \rangle & -\|P \times Q\| & 0 \\ \|P \times Q\| & \langle P, Q \rangle & 0 \\ 0 & 0 & 1 \end{pmatrix}$$

Having this we only need to find a suitable basis to apply this rotation in the desired way. For this we make use of the fact that $P \times Q$ is orthogonal to P and Q and forms a right-handed system. To apply the rotation above we need an ONB. This can be constructed in two steps

- a) Compute $P \times Q$ to get $(P, Q, P \times Q)$. Here P and Q are not orthogonal
- b) Compute $(P \times Q) \times P = Q - \langle P, Q \rangle P$

Now the desired ONB is given by $\left(P, \frac{Q - \langle P, Q \rangle P}{\|Q - \langle P, Q \rangle P\|}, \frac{P \times Q}{\|P \times Q\|} \right)$. Using the change of basis formula with base change matrix $F = \begin{pmatrix} P & \frac{Q - \langle P, Q \rangle P}{\|Q - \langle P, Q \rangle P\|} & \frac{P \times Q}{\|P \times Q\|} \end{pmatrix}$ our rotation will be given by

$$Rot = FGF^{-1}$$

5.2 Convex sets in \mathbb{RP}^2 from tilings

Before we start it is important to note that we will only deal with triangles here. Even though the theory allows us to consider suitable n -gons it is by far the nicest and easiest case to use triangles since we act mostly in \mathbb{R}^3 .

To understand this let us take a look at our setting:

Given a triangle T we want to construct the convex set which is the union of the orbits of the triangle reflection group $\Delta(a, b, c)$ for interior angles $\pi/a, \pi/b, \pi/c$ with $a, b, c > 2$.

The reflections are given in the form $R(x) = \text{Id} - \alpha \otimes v$.

So first of all consider the reflections R_1, R_2, R_3 defined by α_i, v_j for $i, j \in \{1, 2, 3\}$. Due to theorem 3.5 it is sufficient that $\alpha_i(v_j)\alpha_j(v_i) = 4 \cos^2 \left(\frac{\pi}{m_{i,j}} \right)$ where $m_{i,j} \in \{a, b, c\}$ whenever the two sides intersect.

Because the edges of T then correspond to the kernels of the α_i we can and should choose $T = (e_1, e_2, e_3)$ where the e_i are the standard basis of \mathbb{R}^3 . Through this we have the following:

$$\alpha_i = e_i^T \quad v_1 = \begin{pmatrix} 2 \\ v_1^2 \\ v_1^3 \end{pmatrix} \quad v_2 = \begin{pmatrix} v_2^1 \\ 2 \\ v_2^3 \end{pmatrix} \quad v_3 = \begin{pmatrix} v_3^1 \\ v_3^2 \\ 2 \end{pmatrix}$$

where, for example, $v_1^2 v_2^1 = 4 \cos^2 \left(\frac{\pi}{a} \right)$. Since we need explicit values to work with we set in this case $v_1^2 = 1$ and obtain $v_2^1 = 4 \cos^2 \left(\frac{\pi}{a} \right)$.

We thus have our triangle T and all the needed information encoded into the α_i and v_j . Now only three steps remain:

- 1) Generate the group using the R_i as generators. Most times it is enough to compute words up to length 8,
- 2) For each γ in the group compute $\gamma(T)$ and project it onto a suitable affine plane like it is described in the last section,
- 3) Compute the convex hull to get an approximation of the boundary.

If you want to generate images using color here are two ideas that can improve your visualization:

- i) consider building the triangle group and not the triangle reflection group, i.e. use rotations like $S_1 = R_1 R_2$ as generators. In our case the representations would look like this

$$\begin{aligned} \text{triangle reflection group: } & \{R_1, R_2, R_3 | R_i^2 = 1, (R_1 R_2)^a = (R_2 R_3)^b = (R_3 R_1)^c = 1\} \\ \text{triangle group: } & \{x, y, z | x^a = y^b = z^c = 1, xyz = 1\} \end{aligned}$$

where $x = (R_1 R_2), y = (R_2 R_3), z = (R_3 R_1)$.

Then we essentially only draw every second triangle which results in a cleaner image.

- ii) Filter words/triangle: it is likely that some words are actually the same. Thus, to save computation time, it is good to filter words beforehand. On the other hand one can also first compute all triangles and then remove duplicates by checking if two triangles only differ by a small ε (at each vertex). This also gives us a cleaner image especially if we work with opacity since we have no overlap.

5.3 Convex sets in \mathbb{RP}^2 from flags

First of all we want to describe how we can construct a pair of nested triangles given their triple ratio \mathbb{T} . This way we will build a kind of “nice” model pair (Δ, Δ') .

Given a triple of flags $(F_1, F_2, F_3) \in \mathcal{F}_3^+$ the picture is the following:

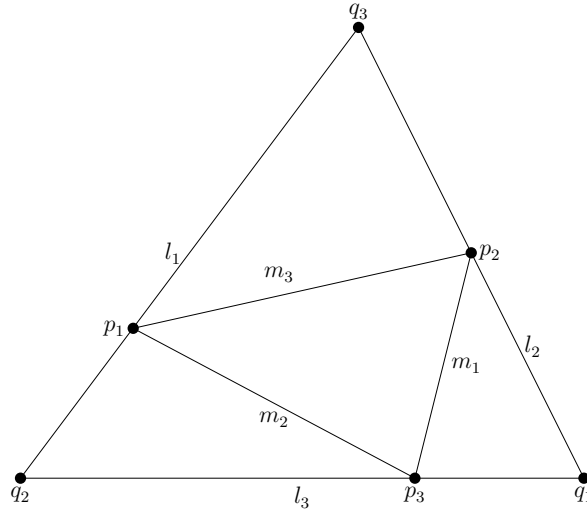


Figure 5.1: Initial setup

where the $(q_i)_i$ are again the intersections of the flags. If we choose the basis (q_1, q_2, q_3) the coordinates of the $(p_i)_i$ become:

$$l_i = e_i^T \quad p_1 = \begin{pmatrix} 0 \\ a \\ b \end{pmatrix} \quad p_2 = \begin{pmatrix} c \\ 0 \\ d \end{pmatrix} \quad p_3 = \begin{pmatrix} e \\ f \\ 0 \end{pmatrix}.$$

Which gives us $\mathbb{T} = T(F_1, F_2, F_3) = \frac{cfb}{eda}$. So choosing the $(p_i)_i$ such that the ratio of the non-zero entries is the same, i.e. \mathcal{T} we obtain

$$\mathbb{T} = \mathcal{T}^3 \quad p_1 = \begin{pmatrix} 0 \\ a \\ a\mathcal{T} \end{pmatrix} \quad p_2 = \begin{pmatrix} d\mathcal{T} \\ 0 \\ d \end{pmatrix} \quad p_3 = \begin{pmatrix} e \\ e\mathcal{T} \\ 0 \end{pmatrix}$$

This is nice for theoretical observations but to draw pictures it is better to have an even easier representation. Thus using convex combinations

$$p_1 = \begin{pmatrix} 0 \\ t \\ 1-t \end{pmatrix} \quad p_2 = \begin{pmatrix} 1-t \\ 0 \\ t \end{pmatrix} \quad p_3 = \begin{pmatrix} t \\ 1-t \\ 0 \end{pmatrix} \quad (5.1)$$

we get $t = 1/(\mathcal{T} + 1)$.

So in short:

- 1) given a desired triple ratio $\mathbb{T} > 0$ compute $\mathcal{T} = \sqrt[3]{\mathbb{T}}$
- 2) compute the points in equation 5.1 for $t = 1/(\mathcal{T} + 1)$

If we want to draw the quadrilaterals we know that the needed intersection points are the classes

$$u_1 = \begin{bmatrix} 1 \\ 1/\tau \\ \tau \end{bmatrix} \quad u_2 = \begin{bmatrix} \tau \\ 1 \\ 1/\tau \end{bmatrix} \quad u_3 = \begin{bmatrix} 1/\tau \\ \tau \\ 1 \end{bmatrix}$$

for $\tau = t/(1 - t)$.

Through this construction we can get a very nice and symmetric triangle for a given triple ratio.

List of Figures

2.1	A flag and two pairs of transverse flags.	9
2.2	Important notation for cross/triple ratio in \mathcal{F}_3 (t_1, t_3 omitted).	10
2.3	Cross ratio connected to triple ratio	11
2.4	$0 < F \in \mathcal{F}_3$ and coloured components of $\mathbb{RP}^2 \setminus (l_2 \cup l_3)$	12
2.5	nested triangles and decomposition for triple of flags	13
2.6	Suitably nested polygons with corresponding flags.	14
2.7	Nested triangles in \mathcal{F}_3^+	14
2.8	Nested triangles in \mathcal{F}_4^+	15
2.9	N' (black), N (blue), I_T (red) and Θ_T (green).	15
2.10	Parameters of \mathcal{F}_4^+ . Red marks newly used information and green the resulting information. Read from left to right.	16
3.1	Tiling generated by a (3,3,4) triangle group	19
3.2	Tiling generated by a (5,7,9) triangle group	19
3.3	Convex set created from eight flags.	19
3.4	Intersecting hyperplanes with basis	22
3.5	Tiling generated by a (4,4,4) triangle reflection group. The depths shown are 1,2,4,6 and 9. Normal vector for affine plane is (1, 4, 5).	25
3.6	Tiling generated by a (3,3,4) triangle group. The depths shown are 1,5 and 10. Normal vector for affine plane is (1, 1, 1).	26
3.7	Tiling generated by a (4,8,12) triangle group. The depths shown are 1,3,6,8 and 12. Normal vector for affine plane is (0.5, 4, 5).	27
3.8	N in blue and N' in black.	28
3.9	Convex sets as boundaries of a union of orbits, drawn with initial n -gon. Shown are values $n = 4, 5, 6, 7, 8, 9$. Flags are drawn in a light gray.	29
3.10	Ideal triangles/5-gon in \mathbb{H}^2 and ideal tetrahedron in \mathbb{H}^3	30
3.11	Cutting up a suitably nested polygon to compute its volume.	31
3.12	Setting around a point p with two reflections.	32
3.13	The spheres S, S' and $S \cap N, S' \cap N$ shown in orange and red. On the right we have the upper half space model with p being mapped to ∞	32
3.14	Construction of convex set via flags. Each level is differently coloured. This is a 6-gon, 4 levels deep.	33
3.15	Construction of convex set via flags. Each level is differently coloured. This is a 7-gon, 4 levels deep.	33
4.1	Nested triangle in a triple of flags $F \in \mathcal{F}_3^+$ and partition into quadrilaterals plus triangle.	35
4.2	Triple of flags with triple ratio 1 and its eruptions for values $t = 1, 2.5, 5$. $\Delta(t)$ in red and $T(t)$ in green.	36
4.3	Triangle T for triple ratio 1 and erupting a hundred times with $t = 0.2$ (left) or $t = -0.2$ (right).	37

4.4	Decomposition of $F \in \mathcal{F}_4^+$ into (N, N') with triangulation.	38
4.5	Initial $F \in \mathcal{F}_4^+$, shearing deformation and bulging deformation. 25 times deformed with $t = 0.1$ (red over green and purple to red).	40
4.6	Initial $F \in \mathcal{F}_4^+$. First image is shear and bulge in each step with $t = 0.1$. Second is bulge with $t = 0.2$, shear with $t = 0.1$ and third is bulge with $t = 0.1$, shear with $t = 0.2$	41
4.7	N_L, N'_L (orange), N_R, N'_R (green) and $a_{1,4}$ (yellow)	42
4.8	Decomposition into four polygons for $i, j, k = 1, 3, 7$	43
4.9	N'_1 in blue with M'_1 less opaque. Same for N'_2 (green) and N'_3 (orange)	43
4.10	Eruptions on a 7-gon in \mathcal{F}_7^+ associated to the drawn triangle for $t = 2, 4, 6, 8$. The last two images show all values at once.	44
4.11	Eruptions on a 7-gon in \mathcal{F}_7^+ associated to all triangles for $t = 0.2, 0.4$	45
4.12	Bulging of a 6-gon at all internal edges with $t = 0.5$. The colours show the deformation after using 1,2 or all 3 internal edges (red to blue).	46
4.13	Eruption flow on \mathcal{F}_3^+ visualized in 3D.	46
4.14	Notation on a convex set with C^1 -boundary. $[\xi(x), \xi(y)]_{\xi(z)}$ in blue.	47
4.15	Data for shearing and bulging flow on convex sets with C^1 boundary. $\Omega_{x,y,L}$ in blue and $\Omega_{x,y,R}$ in green.	48
4.16	Shearing (left) and bulging associated to the drawn line.	49
4.17	Data for eruption flow on convex sets with C^1 boundary.	50
4.18	Eruption flow on convex sets with C^1 boundary for $t = 0$ to $t = 4$ (red to blue).	51
4.19	Eruption flow on convex sets with C^1 boundary for $t = -6$ to $t = 6$. We include this image just because it looks nice.	51
4.20	Applying the a bulge transformation associated to the red line will change the inner parameters of the gray 4-gon but not of the blue 4-gon.	52
4.21	Decomposition of $F \in \mathcal{F}_4^+$ with triangulation and internal edge.	53
4.22	Deforming the nested 4-gons in a suitable chart. N in black, $R_1(N)$ in blue . .	54
4.23	Transforming the red convex set by applying transformations associated to the black edges. Top: bulge, left: shear, right: bulge and shear. Each 10 times for $t = 0$ to $t = 0.9$ (red to green to purple).	56
4.24	Eruption flow on a 9-gon associated to one triangle. Drawn for $t = 0, 0.3, 0.5$ (red, green, blue).	57
5.1	Initial setup	62

Bibliography

- [Ben60] Jean-Paul Benzécri. Sur les variétés localement affines et localement projectives. *Bull. Soc. Math. France*, 88:229–332, 1960.
- [Ben09] Yves Benoist. Five lectures on lattices in semisimple Lie groups. In *Géométries à courbure négative ou nulle, groupes discrets et rigidités*, volume 18 of *Sémin. Congr.*, pages 117–176. Soc. Math. France, Paris, 2009.
- [BK53] Herbert Busemann and Paul J. Kelly. *Projective geometry and projective metrics*. Academic Press INC., New York, 1953.
- [Boy] Edmond Boyer. *Projective Geometry: A Short Introduction*. Online: <http://morpheo.inrialpes.fr/people/Boyer/Teaching/M2R/geoProj.pdf>. [Online; accessed 04-09-2018].
- [Cas15] Bill Casselman. *Essays on Coxeter groups*. Online: <https://www.math.ubc.ca/~cass/research/pdf/Reflections.pdf>, 2015. [Online; accessed 19-03-2018].
- [FG07] V. V. Fock and A. B. Goncharov. Moduli spaces of convex projective structures on surfaces. *Adv. Math.*, 208(1):249–273, 2007.
- [Gol90] William M. Goldman. Convex real projective structures on compact surfaces. *J. Differential Geom.*, 31(3):791–845, 1990.
- [Mar17] Ludovic Marquis. Coxeter group in Hilbert geometry. *Groups Geom. Dyn.*, 11(3):819–877, 2017.
- [Ver04] C. Vernicos. *Introduction aux géométries de Hilbert*. Actes de Séminaire de Théorie Spectrale et Géométrie Vol 23 p.145–168, 2004.
- [WZ18] Anna Wienhard and Tengren Zhang. Deforming convex real projective structures. *Geom. Dedicata*, 192:327–360, 2018.